Diabetologia Springer

Parental high fat diet inhibits glucose-stimulated insulin secretion in the offspring islets of FFA1 knockout mice

Journal:	*Diabetologia*
Manuscript ID	Draft
Manuscript Type:	Article
Keywords:	2.01 Animal - mouse, 3.02.03 Insulin secretion in vitro, 3.02.06 Islet development, 4.01 K/O mice, 2.12 Cell lines, 3.02.01 Islets

Diabetologia checklist for preclinical studies

Adapted from the Animal Research: Reporting of In Vivo Experiments (ARRIVE) Guidelines Checklist [1, 2] and the NIH Principles and Guidelines for Reporting Preclinical Research [3]

	ITEM	RECOMMENDATION	Page no.
Title	1	Provide as accurate and concise a description of the content of the article as possible.	1
Abstract	2	Provide an accurate summary of the background, research objectives, including details of the species or strain of animal used, key methods, principal findings and conclusions of the study.	2-3
INTRODUCTION			
Background	3	a. Include sufficient scientific background (including relevant references to previous work) to understand the motivation and context for the study, and explain the experimental approach and rationale. b. **Animal studies only:** Explain how and why the animal species and model being used can address the scientific objectives and, where appropriate, the study's relevance to human biology.	4-5
Objectives	4	Clearly describe the primary and any secondary objectives of the study, or specific hypotheses being tested.	5
METHODS			
Ethics statement	5	Indicate the nature of the ethical review permissions, relevant licences (e.g. Animal [Scientific Procedures] Act 1986), informed consent, and national or institutional guidelines for the care and use of animals, or for the use of human tissue, that cover the research.	6
Study design	6	For each experiment, give brief details of the study design including: a. The number of experimental and control groups. b. Any steps taken to minimise the effects of subjective bias when allocating animals, cells or tissue samples to treatment (e.g. randomisation procedure) and when assessing results (e.g. if done, describe who was blinded and when). c. The experimental unit (e.g. a single animal, group or cage of animals; single cell). A time-line diagram or flow chart can be useful to illustrate how complex study designs were carried out.	6-8
Experimental procedures	7	**Animal studies only** For each experiment and each experimental group, including controls, provide precise details of all procedures carried out. For example: a. How (e.g. drug formulation and dose, site and route of administration, anaesthesia and analgesia used [including monitoring], surgical procedure, method of euthanasia). Provide details of any specialist equipment used, including supplier(s). b. When (e.g. time of day). c. Where (e.g. home cage, laboratory, water maze). d. Why (e.g. rationale for choice of specific anaesthetic, route of administration, drug dose used).	6-8 and ESM methods
	8	**Cell lines only:** Report the source, authentication and mycoplasma contamination status [3].	
	9	**Studies involving antibodies:** Report source, characteristics, dilutions and how antibodies were validated [3].	ESM methods

Experimental animals	10	**Animal studies only** a. Provide details of the animals used, including species, strain, sex, developmental stage (e.g. mean or median age plus age range) and weight (e.g. mean or median weight plus weight range). b. Provide further relevant information such as the source of animals, international strain nomenclature, genetic modification status (e.g. knock-out or transgenic), genotype, health/immune status, drug or test naive, previous procedures, etc.	7 ESM methods: 1
Housing and husbandry	11	**Animal studies only** Provide details of: a. Housing (type of facility e.g. specific pathogen free; type of cage or housing; bedding material; number of cage companions). b. Husbandry conditions (e.g. breeding programme, light/dark cycle, temperature, type of food, access to food and water, environmental enrichment). c. Welfare-related assessments and interventions that were carried out prior to, during, or after the experiment.	7 ESM methods: 1
Sample size	12	a. Specify the total number of animals or samples used in each experiment, and the number of animals or samples in each experimental group. b. Explain how the number of animals or samples was arrived at. Provide details of any sample size calculation used. c. Indicate the number of independent replications of each experiment, if relevant, e.g. the number of times a western blot was performed. d. Provide sufficient information on sample collection to allow a clear distinction between independent biological data points and technical replicates.	Figure legend (21-22) and ESM Figure legend
Allocating animals/samples to experimental groups	13	a. Give full details of how animals or samples were allocated to experimental groups, including randomisation or matching if done. b. Describe the order in which the animals/samples in the different experimental groups were treated and assessed.	8
Experimental outcomes	14	Clearly define the primary and secondary experimental outcomes assessed (e.g. cell death, molecular markers, behavioural changes).	6-8
Statistical methods	15	a. Provide details of the statistical methods used for each analysis. b. Specify the unit of analysis for each dataset (e.g. single animal, group of animals, single islet). c. Describe any methods used to assess whether the data met the assumptions of the statistical approach. d. Give details of how data are reported, e.g. mean ± SD, median IQR.	8 and Figure legends
RESULTS			
Baseline data	16	**Animal studies only** For each experimental group, report relevant characteristics and health status of animals (e.g. weight, microbiological status, and drug or test naive) prior to treatment or testing. (This information can often be tabulated).	N/A
Numbers analysed	17	a. Report the number of animals or samples in each group included in each analysis. Report absolute numbers (e.g. 10/20, not 50% [4]). b. If any animals or data were not included in the analysis, explain why.	Figure legends
Outcomes and estimation	18	Report the results for each analysis carried out, with a measure of precision (e.g. standard error or confidence interval).	Figure legends
Adverse events	19	**Animal studies only** a. Give details of all important adverse events in each experimental group. b. Describe any modifications to the experimental protocols made to reduce adverse events.	N/A

DISCUSSION			
Interpretation/ scientific implications	20	a. Interpret the results, taking into account the study objectives and hypotheses, current theory and other relevant studies in the literature. b. Comment on the study limitations including any potential sources of bias, any limitations of the animal or model, and the imprecision associated with the results [4]. c. Describe any implications of your experimental methods or findings for the replacement, refinement or reduction of the use of animals in research.	14-16
Generalisability/ translation	21	Comment on whether, and how, the findings of this study are likely to translate to other species or systems, including any relevance to human biology.	16
Funding	22	List all funding sources (including grant number) and the role of the funder(s) in the study.	17

- Please note all queries taken or adapted from the ARRIVE guidelines, except where otherwise indicated.
- Some items are indicated as being specific to certain types of research, e.g. animal studies, studies on cell lines. Please indicate 'N/A' (not applicable) for items that do not apply to your study.

References

1. Kilkenny C, Browne WJ, Cuthill IC, Emerson M, Altman DG (2010) The ARRIVE guidelines checklist. Animal Research: Reporting In Vivo Experiments. Available from www.nc3rs.org.uk/arrive-guidelines, accessed 29 September 2016
2. Kilkenny C, Browne WJ, Cuthill IC, Emerson M, Altman DG (2010) Improving bioscience research reporting: the ARRIVE guidelines for reporting animal research. *PLoS Biol* 8: e1000412.
3. National Institutes of Health (NIH) (2014) Principles and guidelines for reporting preclinical research. Available from www.nih.gov/research-training/rigor-reproducibility/principles-guidelines-reporting-preclinical-research, accessed 29 February 2016
4. Schulz KF, Altman DG, Moher D, the CONSORT Group (2010) CONSORT 2010 Statement: updated guidelines for reporting parallel group randomised trials. *BMJ* 340:c332.

Parental high fat diet inhibits glucose-stimulated insulin secretion in the offspring islets of FFA1 knockout mice

Estela Lorza-Gil[1,2,3], Gabriele Kaiser[1,2,3], Christopher Carlein[4], Markus D.A. Hoffmann[4], Gabriele M König[6], Sieglinde Haug[3], Leticia Prates Roma[4], Elisabeth Rexen Ulven[5], Trond Ulven[5], Evi Kostenis[6], Andreas L. Birkenfeld[1,2,3], Hans-Ulrich Häring[1], Susanne Ullrich[1,2,3*] and Felicia Gerst[1,2,3* #]

[1]German Center for Diabetes Research (DZD e.V.); [2]Institute for Diabetes Research and Metabolic Diseases of the Helmholtz Zentrum München at the University of Tübingen (IDM); [3]Department of Internal Medicine, Endocrinology, Diabetology and Nephrology, University Hospital Tübingen, Tübingen, Germany; [4]Department of Biophysics Faculty of Medicine, Saarland University, Homburg, Germany; [5]Department of Drug Design and Pharmacology, University of Copenhagen, Copenhagen, Denmark; [6]Institute of Pharmaceutical Biology, Bonn University, Bonn, Germany

# corresponding author; *equally contributed

PD Dr. Felicia Gerst
Universitätsklinikum Tübingen
Institut für Diabetes Forschung und Metabolische Krankheiten des HelmholtzZentrum München an der Universität Tübingen (IDM)
Otfried-Müller-Strasse 1072076
Tübingen
Germany

e-mail: felicia.gerst@med.uni-tuebingen.de

Short title: Parental high fat diet, offspring GSIS, FFA1 knockout mice
4477 words

Aims/hypothesis

Neonatal islets aquire glucose-responsive insulin secretion progressively after birth, a process subjected to maternal imprinting. Although non-esterified long chain fatty acids (NEFA) are major components of breastmilk and insulin secretagogues, their role for functional maturation of neonatal beta cells has not been clarified yet. NEFA are the endogenous ligands of fatty acid receptor 1 (FFA1), a Gq-coupled receptor with stimulatory effects on insulin secretion. This study investigates the role of FFA1 in neonatal beta cell function and in the adaptation of offspring beta cells to parental high fat feeding.

Methods

WT and FFA1 KO mice were fed high fat (HFD) or chow diet (CD) for 8 weeks before mating, during gestation and lactation. Blood parameters, pancreas weight and insulin content were assessed in 1, 6, 11 and 26d old (P1-P26) offspring. Beta cell mass and proliferation were determined in P1-P26 pancreatic tissue sections. FFA1/Gq dependence of insulin secretion was evaluated in isolated islets and INS-1E cells using pharmacological inhibitors and siRNA strategy. Transcriptome analysis was conducted in isolated islets.

Results

Blood glucose level of CD FFA1 KO P6 offspring was higher compared to CD WT P6 offspring. Accordingly, glucose-stimulated insulin secretion (GSIS) as well as exendin-4 and palmitate-mediated potentiation were severly impaired in CD FFA1 KO P6-islets. In CD WT P6-islets insulin secretion was stimulated 6-fold by glucose and 5-fold over GSIS by exendin-4 and palmitate, respectively. Although parental HFD increased blood glucose in WT P6 offspring, it had no significant effect on insulin secretion from WT P6-islets. In contrast, parental HFD completely abrogated GSIS in FFA1 KO P6-islets.

Inhibition of Gq by FR900359 or YM254890 in WT P6-islets mimicked the effect of *Ffar1* deletion, i.e. suppression of GSIS and palmitate-augmented insulin secretion. On the contrary, blockage of Gi/o by pertussis toxin (PTX) boosted (20-fold) GSIS in WT P6-islets and rendered FFA1 KO P6-islets glucose responsive, unmasking a constitutive activation of Gi/o. Notably, FR900359 drastically reduced (90%) the positive effect of PTX on GSIS in WT P6-islets, while in FFA1 KO P6-islets FR900359 abolished GSIS in the presence of PTX.

The secretory defect of FFA1 KO P6-islets did not originate from insufficient beta cells, since beta cell mass increased with offspring's age irrespective of genotype and diet. However, during the period of breastfeeding, offspring beta cell proliferation and pancreatic insulin content displayed a genotype- and diet-driven dynamic. The highest proliferation rates were reached under CD at P6 by the KO offspring, and under HFD at P11 by the WT and KO offspring. Only WT offspring was able to adjust, i.e. to increase its pancreatic insulin content following parental HFD.

Conclusions/interpretation

FFA1 promotes the gain of glucose-responsive insulin secretion in newborn islets and is required for adaptive offspring insulin secretion to parental HFD.

Research in context

What is already known about this subject?

- Neonatal beta cells undergo a series of transcriptional and signalling adaptations to achieve glucose-responsive insulin secretion, a process known as functional maturation
- Functional maturation of neonatal islets occurs during breastfeeding age and is largely accomplished by the time of weaning, which is why the maternal environment is essential for the offspring islets
- Maternal obesogenic/diabetogenic diet increases type 2 diabetes risk in offspring

What is the key question?

- Does free fatty acid receptor 1 (FFA1) play a role for the functional maturation of neonatal beta cells?

What are the new findings?

- FFA1 promotes the gain of glucose-responsive insulin secretion in the neonatal islets
- FFA1 is necessary for the ability of the offspring to adapt its insulin secretion, insulin content and beta cell mass to the parental high fat diet-induced metabolic stress
- Neonatal glucose-stimulated insulin secretion as well as GLP-1R-augmented insulin secretion depend on active Gq

How might this impact on clinical practice in the foreseeable future?

- Pharmacological modulation of FFA1/Gq signalling might protect offspring islets from adverse effects induced by maternal obesity and/or gestational diabetes

Introduction

Obesity, a major risk factor for type 2 diabetes (T2D), requires enhanced insulin production and adaptive insulin hypersecretion. The failure of pancreatic beta cells to cope with such high insulin demand results in relative insulin deficiency, which is the ultimate cause for chronic hyperglycaemia and overt T2D in humans [1-3].

Glucose stimulated insulin secretion (GSIS), the main functional trait of healthy beta cells, is not fully developed in newborn islets. Glucose responsiveness gradually develops in beta cells during early postnatal life, and this process is imperative for adequate adult beta cell function. As a matter of fact, insulin secretion of newborn islets is poorly glucose responsive, being mainly driven by amino acids [4-6]. The ability of adult beta cells to adjust their function to the metabolic requirements is tailored very early in life by the intrauterine and by the neonatal environment, i.e. maternal metabolism and breastmilk feeding [7-9]. The consequences of maternal obesogenic/diabetogenic diet for the metabolic plasticity of offspring beta cells and the progeny's risk to develop diabetes are not yet fully understood [10-12]. In rodents, high fat diet (HFD) administration during pregnancy and lactation resulted in increased body weight and beta cell mass, fasting hyperinsulinemia, hyperglycaemia and glucose intolerance in offspring [13-15]. Consistent with these findings in animal models, maternal obesity in humans is associated with increased incidence of T2D in offspring [16].

The role of non-esterified long chain fatty acids (NEFAs), major components of breast milk [17] and insulin secretagogues, for functional maturation of neonatal beta cells remains elusive. NEFAs areendogenous agonists of free fatty acid receptor 1 (FFA1), a Gq/11-coupled receptor (GPCR) that stimulates insulin secretion [18, 19]. The function and the signalling pathways of GPCRs have been extensively studied in adult beta cells. Thus, Gs- and Gq/11-coupled receptors stimulate, while PTX-sensitive Gi/Go-coupled receptors inhibit insulin secretion. Gs-coupled glucagon-like peptide-1 receptor (GLP1R) emerged as a powerful tool for T2D treatment [20]. In spite of its positive effects on GSIS, FFA1 has not yet overcome the burdens of clinical trials. Nevertheless, both GLP1R and FFA1 potentiate GSIS in a glucose-dependent manner, a therapeutic prerequisite to avoid hypoglycaemic episodes [21].

While various GPCR can share one type of G protein, there is increasing evidence that a receptor can recruit varius G proteins. Gq is the major G protein recruited by FFA1

in adult beta cells, but a certain degree of promiscuity for G proteins, i.e. Gs or G12/13 was ascribed to FFA1, depending on ligand and cellular system [22, 23]. In a similar manner, GLP1R, that augments insulin secretion via Gs-mediated stimulation of adenylate cylase, can couple to Gq and in that way sustain insulin secretion under hyperglycaemic conditions. Thus, in beta cells exposed to metabolic stress Gq-mediated signalling acts as a potent stimulator of GSIS [24].

GPCRs also modulate beta cell survival and proliferation. While Gi/oPCRs reduce beta cell proliferation, both GLP1R and FFA1 promote beta cell survival and thereby the maintenance of beta cell mass [25-27]. Distinct to adult beta cells with their extremely low proliferation rate, neonatal beta cells are responsive to proliferative cues, therefore neonatal proliferation impacts on adult beta cell mass. Although a positive effect of NEFAs on neonatal beta cell proliferation has been described, a role of FFA1/Gq in this is unclear [28].

The aim of the present study is to understand the role of FFA1 and Gq for proliferation and functional maturation, i.e. gain of glucose responsiveness of neonatal beta cells in the context of an obesogenic parental diet.

Methods

All animal experiments were approved by the local authorities (Approval No. M10-18G of the Regional Council Tübingen, Germany). Animal care and handling was conducted in compliance with the German law for the protection of animals used for scientific purposes and in accordance with ARRIVE guidelines.

Mouse model and feeding

C57BL/6-RipCre-ROSA$^{mT/mG}$ WT and FFA1 KO animals were generated as described in the ESM methods. The islets of these mice display an insulin secretion similar to that of WT and FFA1 KO C57BL/6 mice, respectively (ESM Fig. 1c-e).

WT and FFA1 KO animals (4 weeks old) were randomly asigned to chow (CD) or high fat diet (HFD) and fed accordingly 8 weeks before mating (Fig. 1a). WT and FFA1 KO breeding pairs were kept on the respective diet throughout pregnancy and lactation period. Offspring animals (21d old) were weaned on CD. Offspring was examined at postnatal days 1, 6, 11, and 26 (P1-P26). Blood samples were taken immediately after sacrification. Blood parameters were determined as described in ESM methods. Whole pancreas was resected, weighed and processed as described below.

Offspring beta cell mass and proliferation

P1-P26 offspring pancreata were fixed in 4% formalin, dehydrated (10-30% sucrose in PBS), embedded in Tissue-Tek® O.C.T. compound (Sakura Finetek) and cut into serial 10 µm cryosections. Whole section panorama images (6-10 sections/pancreas) were captured at 10x magnification using an ApoTome System (Zeiss). Pancreatic area (red fluorescence) and insulin-positive area (green fluorescence) were determined using Fiji (open-source distribution of ImageJ; version 1.48d). Beta cell mass (mg) was calculated by multiplying relative beta cell area ((GFP-positive)/pancreas area (Tomato-positive)) by pancreas weight (mg).

For assessment of beta cell proliferation cryosections were permeabilized (0.2% Triton-X-100 in PBS), blocked with 10% FCS-PBS, incubated with anti-Ki67 antibody (1:200), followed by incubation with 2nd fluorocrome-coupled antibody (Alexa-Fluor633 IgG, 1:1000). Nuclei were stained with DAPI. Beta cell proliferation was calculated as % of Ki67/GFP-positive of GFP-positive cells.

Offspring pancreatic insulin content

P1-P26 offspring pancreata were isolated, weighed and imediately minced in ice-cold acid ethanol (1.5% (v/v) HCl in 75% (v/v) ethanol) for the extraction of total pancreatic insulin. Insulin was quantified using insulin ELISA (Mercodia).

Mouse islet isolation

P6-/P11-offspring pancreata were minced in collagenase solution (0.5 mg/ml, NB8, Serva) and digested for 20 min at 37ºC. Islets from the adult mice were isolated by collagenase injection (1 mg/ml) into the pancreas followed by digestion for 10 min at 37ºC. Islets were washed with Hank's balanced salt solution (see ESM method) supplemented with 0.5 % BSA (fraction V; Sigma) and collected by hand picking. The islets were cultured overnight as described in ESM methods.

Insulin secretion

Isolated islets were preincubated for 1h in Krebs Ringer buffer (KRB; see ESM methods) containing 2.8 mM glucose, then incubated for 1h in KRB containing 2.8 or 12 mM glucose and test substances as indicated. Pertussis toxin (100 ng/ml) was added for 18-20 h during culture. Palmitate (60 µM at 0.05% BSA and 600 µM at 0.5% BSA), TUG-469 (FFA1 agonist, 10 µM at 0.05% BSA), exendin-4 (100 nM) and forskolin (1 µM) were added during the 1h incubation. Gq inhibitors FR900359 (1 µM) and YM-254890 (100 nM), H1152 (ROCK inhibitor, 1µM) were added to the pre-/incubation buffers, CT3 toxin (RhoA inhibitor, 2 µg/ml) was added to culture medium 2h previous to and during the secretion assay. Secreted insulin and insulin content after extraction in acid ethanol (1.5% (v/v) HCl in 75% (v/v) ethanol) were measured by ELISA (Mercodia).

INS-1E cell culture, siRNA treatment, RNA isolation and Western blotting

INS-1E cells cultured under standard conditions weretransfected with 20 nM non-targeting siRNA or Gnaq siRNA and insulin secretion was measured 3d after transfection (ESM methods). Control and transfected INS-1E cells were lysed in RNA isolation buffer or RIPA buffer (ESM methods) as described previously [30]. Cellular proteins were separated on 10% SDS-PAGE and blotted on nitrocellulose membrane. Membranes were blocked with 5% milk-TBS containing 0.15% Tween, incubated with anti-Gq Ab (1:1000) and HRP-labelled 2nd antibody (1:2000). Protein bands were visualised with ChemiDoc Touch Imaging System (BioRad Laboratories) and quantified using ImageLab software (version 5.2.1).

RNA isolation, RT-PCR and RNAseq

Isolated islets, INS1 cells, islet cell suspensions and FACS-sorted islet cells were lysed using the Nucleospin RNA isolation kit (Macherey Nagel, Germany). Cellular RNA (0.1 µg) was transcribed into cDNA using the Transcriptor first strand cDNA synthesis kit (Roche Diagnostics). Semi-quantitative PCR was performed with the LightCycler 480

system (Roche Diagnostics) using mouse/rat specific primers (Invitrogen) as listed in ESM Table 1. RNA isolated from CD WT and FFA1 KO P6-offspring islets was subjected to RNAseq analysis as previously described [30].

Immunostaining of INS-1E cells

Cells seeded on poly-ornithine-coated coverslips were pre-incubated for 1h in KRB containing 2.8 mM glucose ± FR900359 (1 µM) and then incubated for 10min in KRB with 2.8 or 12 mM glucose ± palmitate (600 µM). Thereafter the cells were fixed with 4% formalin, permeabilized with 0.2% Triton-X100-PBS, blocked with 10% FCS-PBS, incubated overnight with anti-Gq Ab (1:1000) and for 1h with 2nd fluorochrome-coupled antibody (1:1000; AlexaFluor488 IgG). Nuclei were stained with DAPI. Cells were examined with an ApoTome System (Zeiss) using a 63x objective.

Cytosolic [Ca^{2+}]i measurement

Islets from 12 weeks old C57BL/6N mice were loaded with 2.5 µM Fura-2 AM (F1221; Invitrogen) for 2h. Islets were kept in culture medium during the first h of loading, then were transferred to KRB-Henseleit solution (KHB) supplemented with 0.5% DMSO or FR900359 (1 µM; ESM Methods). The islets were placed in KHB with 2.8 mM glucose and after 5 min baseline recording, glucose concentration was raised to 12 mM and the measuemtent continued for 30 min. KCl (30 mM) was used as a positive control. When pretreatment with Gq inhibitor was ommited, FR900359 or DMSO were added during recording at high glucose. Fluorescence was measured at 500 to 550 nm (BP 525/50 HE) with alternating 340 (BP 340/30) and 380 nm (BP 387/15) excitation using an inverted microscope (10x objective; Axio Observer 7, Zeiss). Images were taken every 2 s for max 45 min. Area under the curve (AUC) was calculated using OriginPro 2022.

Statistical analysis

Data are expressed as mean ± SEM with the number (n) of replicates and independent experiments as indicated. RNAseq data set was processed with the R package DESeq2 v1.22.1. All other results were subjected to statistical ANOVA analysis using GraphPad Prism (version 9.1.2). Differences were considered statistically significant at $p \leq 0.05$. * $p<0.05$, **$p<0.005$, ***$p<0.001$; ****$p<0.0001$. Mice and isolated islets were randomly distributed for analysis. Quantification of histological staining was performed by a trained scientist and the pictures blinded.

Results

Parental HFD feeding abrogates GSIS in Ffar1 deficient offspring

WT and FFA1 KO breeding pairs (F0) were asigned to CD or HFD (Fig. 1a). HFD caused significant weight gain in F0 male mice (ESM Fig. 2a). Neither HFD nor *Ffar1* deletion altered fed blood glucose, triglycerides, leptin and adiponectin levels in F0 mice (ESM Fig. 2a-j). However, HFD induced liver steatosis in WT, and to a lesser extent in FFA1 KO animals, as previously described (ESM Fig. 2k, [31]).

The role of FFA1 in offspring glucose homeostasis was assessed by comparing WT and FFA1 KO offspring mice (F1) at P1-P26; Fig. 1a and ESM Fig. 3). Parental HFD increased blood glucose in WT P6- and P11-offspring but had no impact on plasma glucose of FFA1 KO P6- and P11-offspring (Fig. 1b,c). However, under CD, FFA1 KO P6-offspring had higer plasma glucose than WT P6. This difference was transient, as WT and FFA1 KO P1-, P11-, and P26-mice had similar blood glucose (Fig. 1c and ESM Fig. 3a,b). HFD increased leptin, though not affecting serum adiponectin in FFA1 KO P6 (ESM Fig. 3c,d). Neither parental diet nor *Ffar1* deletion altered offspring body and pancreatic weight (ESM Fig. 3e,f). These results suggest that parental HFD and FFA1 deficiency, the latter irrespective of parental metabolic pressure, transiently impair neonatal *in vivo* glucose homeostasis.

Since increased blood glucose level in offspring may result from impaired beta cell function, we examined insulin secretion in P6- and P11-offspring islets (Fig. 1d-g). In WT P6-islets insulin secretion was increased (4-5 fold) by glucose (12 and 20 mM) irrespective of parental diet (Fig. 1d). CD FFA1 KO P6-offspring islets were less glucose responsive, i.e. only 20 mM glucose elicited a significant stimulation (Fig.1d). Besides, parental HFD abrogated GSIS of FFA1 KO P6-islets, an effect that persisted at P11 (Fig. 1e). Endorsing the role of FFA1 for the neonatal insulin secretion, palmitate increased GSIS in CD WT P6- and P11-islets (5.5- and 3.7-fold, respectively), but failed to augment GSIS in FFA1 KO offspring islets (Fig. 1f,g). The impairment of insulin secretion in KO offspring is not restricted to FFA1 pathway, as exendin-4 (GLP1R agonist) enhanced GSIS of WT P6-islets, whereas its effectiveness was reduced in FFA1 KO P6-islets (Fig. 1f). A poorly functional GLP1R in FFA1 KO P6-offspring islets most probably accounts for their reduced incretin responsiveness, since forskolin, which bypasses GLP1R, maximally stimulated secretion independent of parental diet and genotype (Fig. 1f,g). These results indicate that FFA1 signalling is

required for neonatal GSIS and for the offspring ability to adapt insulin secretion to the parental metabolic stress.

FFA1 KO offspring islets have increased proliferation rate

Since the negative effect of *Ffar1* deletion on GSIS in P6-islets might result from disturbed islet maturation, we performed comparative transcriptome analysis (bulk RNAseq) of CD WT and FFA1 KO P6-islets. We found only 24 up- and 8 downregulated genes ($+1<Log_2FC<-1$; *p adj* < 0.05) in FFA1 KO islets (Fig. 2a, ESM Fig. 4a, ESM Table 2). With exception of lower *Sst* mRNA level in FFA1 KO P6-islets, the beta cell specific genes, as well as the G protein mRNAs remained largely unaltered by *Ffar1* deletion (ESM Table 2 and ESM Fig. 4a).

Top upregulated and highly expressed genes in FFA1 KO P6-islets were the early-response genes *Fos, Egr1* and *Jun*, known to promote proliferation (Fig. 2a). Interestingly, parental HFD increased expression of *Fos* and *Jun* in WT P6-islets but had an opposite effect on these genes in FFA1 KO P6-islets (Fig. 2b,c).

In addition, the ER stress response genes *Hspa1a, Hspa1b* as well as terms related to cytokines signalling such as *Socs3* and *Dusp1* were upregulated in FFA1 KO P6-islets. Parental HFD increased these mRNAs in WT P6-islets to levels comparable to those of FFA1 KO P6-islets (ESM Fig. 4b-e). In adult islets, the mRNA level of all above mentioned genes was low and not altered by diet or genotype (Fig. 2c,d and ESM Fig 4b-e). Expression of *Ffar1* was not affected by parental diet (Fig. 2d).

Gene ontology (GO) overrepresentation analysis indicated enrichment for terms related to ECM organisation, cytoskeleton, focal adhesion and ER lumen in FFA1 KO P6-islets (ESM Fig. 4g,h). Of note, no termes associated with GPCR pathways, mitochondrial function or cellular metabolism were altered.

The top ranking upregulated gene in FFA1 KO P6-islets ($Log_2FC = 3.99$) was the low abundant *Prodh2* encoding for hydroxyproline dehydrogenase, a mitochondrial enzyme that catabolises 4-hydroxy-proline (Fig. 2a, ESM Fig. 4f). The upregulation of *Prodh2* was diet- and age-independent (ESM Fig. 4f). In accordance with the increased expression of *Prodh2*, 4-hydroxy-proline, but also L-proline, improved GSIS of CD FFA1 KO P6-islets (ESM Fig. 4i). L-proline had no beneficial effect of GSIS in WT P6-islets (ESM Fig. 4j). Thus, the increased expression of PRODH2 in FFA1 KO P6-islets supports the amino acid-responsive insulin secretion, a functional trait of immature beta cells.

Considering the upregulation of proliferative genes in FFA1 KO P6-islets, we quantified beta cell proliferation in P1-P26 offspring pancreata via Ki67 immunostaining (Fig. 2e and ESM Fig. 5). The percentage of proliferating beta cells increased during the breastmilk feeding period, i.e. P1 to P11 and declined in weaned P26-offspring regardless of parental diet and genotype. Notably, under CD, the highest proliferation rate was reached by the FFA1 KO P6-offspring. Under parental HFD, the peak of proliferation rate was shifted toward P11 in both WT and FFA1 KO mice (Fig. 2e).

In parallel, offspring beta cell mass gradually increased from P1 to P26 (Fig. 2f). Although the overall increase was not altered by diet, the quality of this increase was slightly different between genotypes. Thus, in WT offspring beta cell mass reached the highest level at P26. In FFA1 KO offspring beta cell mass stopped increasing further after P11 (Fig. 2f). In parallel to the gain in beta cell mass, pancreatic insulin content steadily increased from P1 to P26. However, as long as the offspring was breast fed, solely the WT offspring was able to adjust, i.e. to increase its insulin content in response to parental HFD (Fig. 2g).

These results show that beta cell maturation and the onset of glucose responsiveness are delayed in FFA1 KO offspring islets. In addition, FFA1 deficiency impairs offspring's ability to adjust beta cell function to maternal HFD during breastfeeding.

GSIS is regulated by G proteins in mouse islets

Since we found no altered expression of genes controlling functional maturation and insulin secretion in FFA1 KO P6-islets, their impaired GSIS is most likely a consequence of disturbed FFA1 signalling. A major branch of FFA1 signalling, involved in stimulation of GSIS, relies on activation of Gq-coupled phospholipase C and generation of IP_3 and DAG, which then increase $[Ca^{2+}]i$ [32].

To assess whether Gq accounts for the stimulatory effect of FFA1 on GSIS in WT P6-islets, we used a specific Gq inhibitor FR900359 (1 μM) which was purified from *Ardisia crenata* leaves as described earlier in detail [33]. In WT P6-islets, FR900359 inhibited palmitate- and TUG-469-amplified insulin secretion, but abolished also GSIS (Fig. 3a). Furthermore, The inhibitory effect of FR900359 on GSIS persisted in the presence of tolbutamide- and exendin-4 in WT P6-islets (Fig. 3b).

Inhibition of GSIS after FFA1 deletion or Gq inhibition may result from derepressed inhibitory pathways, i.e. Gi/Go-mediated inhibition of GSIS [34]. Therefore, we used pertussis toxin (PTX) to specifically inactivate Gi/Go proteins. Pretreatment of WT P6-islets with PTX increased GSIS 100-fold without affecting basal secretion (Fig. 3c).

FR900359 reduced the stimulatory effect of PTX by 90%, suggesting that GSIS largly depends on Gq when Gi/Go signaling is off. Of note, the simultaneous inhibition of Gq and Gi/o (PTX + FR900359) unmasked a 14-fold stimulation of insulin secretion by glucose in WT P6-islets (Fig. 3c). Inactivation of Gi/Go rendered FFA1 KO P6-islets glucose responsive (10-fold stimulation), an effect cancelled by FR900359 (Fig. 3d).

To confirm the role of Gq for neonatal GSIS, a second Gq inhibitor (YM-254890; 100 nM) was tested. YM-254890 recapitulated the effects of FR900359 on glucose and palmitate-stimulated insulin secretion in WT P6-islets (Fig. 3e). Interestingly, both FR900359 and YM-254890 reduced forskolin-stimulated insulin secretion of FFA1 KO P6-islets by 40% (Fig. 3f). These findings confirm a key role of FFA1/Gq signalling for glucose responsiveness and insulin secretion of neonatal islets.

FFA1 can recruit also G12/13, a G protein reported to activate RhoA/ROCK signalling and shape the actin network. Since inhibition of ROCK sustains functional maturation of iPS-derived beta cells [35], we examined the effect of RhoA/ROCK inhibition on GSIS in P6-islets. Inhibition of RhoA with exoenzyme C3 transferase slightly improved glucose responsiveness in FFA1 KO P6-islets (Fig. 4a). In WT P6-islets, RhoA inhibitor neither improved GSIS nor rescued the GSIS after FR900359 treatment (Fig. 4b). The ROCK inhibitor H1152 improved glucose responsiveness in FFA1 KO P6-islets (Fig. 4c). In WT P6-islets H1152 had no effect on GSIS, although the cortical actin web of WT beta cells turned punctured upon H1152 treatment (Fig. 4d, e).

Toghether, these results indicate that GSIS of neonatal mouse islets largely depends on the activity of stimulatory Gq and inhibitory Gi/o.

Downregulation of Gq expression in INS-1E cells mimics the effect of Gq inhibitors

To further confirm the need for Gq for GSIS, we downregulated Gq expression in INS-1E cells. Following Gnaq siRNA treatment, mRNA and protein levels of Gq were reduced by 80% (Fig. 5a-c), and glucose- and palmitate-stimulated insulin secretion were significantly lower than in INS-1E cells transfected with control siRNA (Fig. 5d). Worth mentioning, the GLP1R antagonist exendin-9 lowered GSIS in control INS-1E cells but not in INS-1E cells with downregulated Gq (Fig. 5d). Thus, GSIS of INS-1E cells depends at least partly on active Gq.

In INS-1E cells, glucose stimulated insulin secretion was also inhibited by FR900359 (Fig. 5e). Since FR900359 acts as a potent guanine nucleotide dissociation inhibitor (GDI) for Gq [33] we next used immunostaining to assess whether FR900359

intereferes with the subcellular distribution of Gq. In INS-1E cells exposed to either 2.8 mM or 12 mM glucose ± palmitate (600 µM) we detected Gq-associated fluorescence with a plasma membrane-like distribution (Fig. 5f, upper panels). In the cells treated with FR900359 we found mainly cytosolic residing Gq-associated fluorescence (Fig. 5f, lower panels). Hence, FR900359 interferes with the subcellular distribution of Gq and in this way it may hinder GPCRs to optimally recruit Gq.

GSIS and cytosolic Ca^{2+} of adult islets are sensitive to Gq inhibition

To assess whether dependency of GSIS on Gq is restricted to the neonatal islets, we performed GSIS in FR900359-treated adult WT islets. Similar to the neonatal islets, FR900359 inhibited both GSIS and exendin-4- and palmitate-amplified insulin secretion (Fig. 6a,b). In view of the pronounced effect of FR900359 on GSIS, we tested whether Gq inhibition interferes with the $[Ca^{2+}]i$ in adult WT islets. Although FR900359 reduced the amplitude of $[Ca^{2+}]i$ in respone to 12 mM glucose (17.3% of AUC glucose), it did not interfere with the initial changes of $[Ca^{2+}]i$ induced by glucose (Fig. 6 c,d). Acute addition of FR900359 triggered a fast reduction of $[Ca^{2+}]i$ without affecting the KCl-induced rise in $[Ca^{2+}]i$ (8.3% of AUC glucose; Fig. 6 e,f). These rather small effects of FR900359 on $[Ca^{2+}]i$ may not explain its profound effect on GSIS.

Discussion

In the present study, we investigated the role of FFA1 on offspring islet function during parental imprinting using a well characterized FFA1 KO mouse model [31]. Our findings indicate that FFA1 promotes the gain of glucose-responsive insulin secretion from neonatal islets and is required for adaptive insulin secretion of the offspring to parental HFD. Thus, FFA1 deletion as well as inhibition of Gq impaired glucose- and palmitate-stimulated insulin secretion from P6-islets. Furthermore, parental HFD abolished insulin secretion from the FFA1 KO P6-offspring islets, while neither GSIS nor exendin-4 and palmitate-stimulatedGSIS from WT P6-islets were affected by parental HFD. These observations indicate an important role of FFA1 and Gq signalling for the functional maturation of beta cells.

In functionally mature islets, the effectiveness of glucose stimulation on isulin secretion is modulated by a diversity of GPCRs. The stimulatory effect of Gs-coulped (GLP1R, GIPR, GCGR) and Gq/11-coupled (FFA1 and CHRM3) receptors, and the inhibitory action of Gi/o-coupled ones (ADRA2A, SSTR, GALR) on GSIS are well characterized [36]. Distinct to the GsPCRs, which are targeted by therapies to treat insulin deficiency in T2D, the therapeutic potential of FFA1 remains controvertial [20, 21]. Sassmann et al. described a diminished GSIS in mouse islets with beta cell specific deletion of Gq/11, as consequence of impaired glucose-mediated closure of K_{ATP} channels [37]. In agreement, we showed that Gq inhibitor FR900359 abrogates GSIS in neonatal and adult islets. Moreover, a second Gq inhibitor (YM254890) mimicked the effect of FR900359 on GSIS, and downregulation of Gqα in INS-1E cells impaired GSIS.

Gq inhibition attenuated the plateau phase of glucose-induced rise of $[Ca^{2+}]_i$ in adult mouse islets, but this cannot entirely explain the pronounced effect of FR900359 on GSIS. The initial reduction and the subsequent rise of $[Ca^{2+}]_i$ by glucose were not affected by the preincubation with FR900359, suggesting that the inhibitor exerted no toxic effects on islet cell metabolism. Beside a putative Gq-mediated inhibition of hyperpolarising K^+ channels, the involvement of Gq in Ca^{2+} mobilisation and Ca^{2+}-dependent exocytosis could account for the large impact of Gq inhibitors on insulin secretion [38]. In this sense, DAG generated by GqPCR-activated PLC was showed to interact with the SNARE protein Munc13-1 and to prime the secretory vesicles for exocytosis in chromaffin cells [39]. Moreover, glucagon secretion depends on Gq, and glucagon augments insulin secretion via paracrine activation of GLP1R on beta cells [40, 41]. Therefore, inhibition of Gq may also impair the glucagon/GLP1R-mediated

stimulation of insulin secretion. However, in the beta cell line INS-1E the Gq inhibitor abrogated GSIS, suggesting a direct effect on beta cells.

According to our results, neonatal GSIS is restricted by inhibitory Gi/o. Indeed, PTX-induced inactivation of Gi/o markedly increased neonatal GSIS in a FFA1-independent manner. Of note, this effect of PTX largely depends on Gq, since FR900359 curtailed 90% of the PTX-stimulated GSIS. Such a stimulatory effect of PTX on GSIS has been previously observed in adult mouse islets [42], but not in INS-1E cells (data not shown), suggesting that PTX counteracts an islet intrinsic, possibly somatostatin-mediated inhibition of insulin secretion [43].

The sensitivity of exendin-4 and forskolin-augmented GSIS toward Gq inhibition was surprising and is in disagreement with previous observations [37, 44]. Nevertheless, our results are in accordance with a recent work describing that GLP-1R recruits Gq and thereby rescues insulin secretion of islets exposed to metabolic stress [24]. Whether such a Gs-to-Gq shift is responsible for these discrepant results needs further experimental evidence.

Several lines of evidence indicate that maternal overnutrition impairs offspring beta cell function and increases offspring risk for T2D [10, 11]. We show here that the ability of offspring neonatal islets to adjust their function to parental obesogenic pressure depends on FFA1. Likewise, a loss-of-function mutation of FFA1, occuring at increased frequency in severely obese humans, is associated with impaired $[Ca^{2+}]_i$ and reduced insulin secretion, which points out the importance of FFA1 for adaptive insulin secretion under conditions of lipid overload [45].

Distinct to adult beta cells, neonatal beta cells are proliferative, a feature progresively lost along with the gain of functional competence [46, 47]. According to the RNAseq results, the expression of several beta cell immaturity markers (Sox9, Hes1, Myc) is elevated in FFA1 KO P6-offspring islets, a further indication that FFA1 promotes functional maturation. While both FFA1 deletion and parental HFD increased offspring beta cell proliferation, the quality of their effect was slightly different. Thus, FFA1 deletion increased the proliferative capacity of P6 beta cells, while parental HFD extended the proliferative time window toward P11 in a FFA1-independent manner. In spite of promoting proliferation, FFA1 deletion had negative consequences for expansion of functional beta cell mass, and even more obvious, for the insulin content, especially in the context of neonates' exposure to metabolic stress, i.e. maternal HFD. Of note, among the P6 offspring insulin content was the lowest in the HFD KO group,

the one with the secretion-incompetent islets. These FFA1-related effects were limited to the pre-weaning phase, i.e. exposure to maternal nutrition, as P26 offspring displayed similar proliferation rates, beta cell mass and insulin content irrespective of genotype and parental diet. The lipid-rich neonatal environement may therefore justify the functional relevance of FFA1 during early life, since FFA1 is the main mediator of LCFA effects on GSIS [48, 49]. Whether Gq solely transmits the effects of FFA1 in neonatal islets is, to our knowledge, not known so far. Nevertheless, both Gi and Gs were found to impact on neonatal beta cell proliferation [27, 50].

Based on our results, we postulate that FFA1/Gq signalling promotes GSIS of neonatal beta cells as well as their ability to adapt to parental fat overload. In conclusion, therapeutic modulation of FFA1/Gq signalling might protect from adverse effects of maternal obesity on offspring glucose homeostasis.

Author contributions

SU, FG and ELG designed the experiments. FG, ELG, SG, GK, CC, MDAH, LPR, GMK, ERU and TU performed experiments and analysed data. SU, EV, ALB, HUH contributed to data interpretation. FG and SU drafted the manuscript. All authors approved the final version of the manuscript and have agreed to be personally accountable for the entire study.

FG and ELG are the guarantors of this work, have full access to all data and assume responsibility for the integrity of the data and the accuracy of the data analysis.

Funding

This study was supported by a grant (01GI0925) from the Federal Ministry of Education and Research (BMBF) to the German Center for Diabetes Research (DZD e.V.)

ERU is funded by the Lundbeck Foundation (grant R307-2018-2950). E.K. and G.M.K. gratefully acknowledge support of this work by the DFG-funded Research Unit FOR2372 with the grants 290847012 / FOR2372 (to E.K), as well as 290827466 / FOR2372 (to G.M.K.).

Competing interests

The authors declare no competing interests.

References

[1] Prentki M, Nolan CJ (2006) Islet beta cell failure in type 2 diabetes. J Clin Invest 116: 1802-1812
[2] Weir GC, Bonner-Weir S (2004) Five stages of evolving beta-cell dysfunction during progression to diabetes. Diabetes 53 Suppl 3: S16-S21
[3] Cohrs CM, Panzer JK, Drotar DM, et al. (2020) Dysfunction of Persisting β Cells Is a Key Feature of Early Type 2 Diabetes Pathogenesis. Cell reports 31: 107469
[4] Helman A, Cangelosi AL, Davis JC, et al. (2020) A Nutrient-Sensing Transition at Birth Triggers Glucose-Responsive Insulin Secretion. Cell Metab 31: 1004-1016.e1005
[5] Jermendy A, Toschi E, Aye T, et al. (2011) Rat neonatal beta cells lack the specialised metabolic phenotype of mature beta cells. Diabetologia 54: 594-604
[6] Henquin JC, Nenquin M (2018) Immaturity of insulin secretion by pancreatic islets isolated from one human neonate. Journal of diabetes investigation 9: 270-273
[7] O'Dowd JF, Stocker CJ (2013) Endocrine pancreatic development: impact of obesity and diet. Front Physiol 4: 170
[8] Moullé VS, Parnet P (2019) Effects of Nutrient Intake during Pregnancy and Lactation on the Endocrine Pancreas of the Offspring. Nutrients 11
[9] Stolovich-Rain M, Enk J, Vikesa J, et al. (2015) Weaning triggers a maturation step of pancreatic β cells. Developmental cell 32: 535-545
[10] Nielsen JH, Haase TN, Jaksch C, et al. (2014) Impact of fetal and neonatal environment on beta cell function and development of diabetes. Acta Obstet Gynecol Scand 93: 1109-1122
[11] Jacovetti C, Regazzi R (2022) Mechanisms Underlying the Expansion and Functional Maturation of β-Cells in Newborns: Impact of the Nutritional Environment. Int J Mol Sci 23
[12] Elsakr JM, Gannon M (2017) Developmental programming of the pancreatic islet by in utero overnutrition. Trends Dev Biol 10: 79-95
[13] Nicholas LM, Nagao M, Kusinski LC, Fernandez-Twinn DS, Eliasson L, Ozanne SE (2020) Exposure to maternal obesity programs sex differences in pancreatic islets of the offspring in mice. Diabetologia 63: 324-337
[14] Graus-Nunes F, Dalla Corte Frantz E, Lannes WR, da Silva Menezes MC, Mandarim-de-Lacerda CA, Souza-Mello V (2015) Pregestational maternal obesity impairs endocrine pancreas in male F1 and F2 progeny. Nutrition 31: 380-387
[15] Bringhenti I, Ornellas F, Mandarim-de-Lacerda CA, Aguila MB (2016) The insulin-signaling pathway of the pancreatic islet is impaired in adult mice offspring of mothers fed a high-fat diet. Nutrition 32: 1138-1143
[16] Lahti-Pulkkinen M, Bhattacharya S, Wild SH, et al. (2019) Consequences of being overweight or obese during pregnancy on diabetes in the offspring: a record linkage study in Aberdeen, Scotland. Diabetologia 62: 1412-1419
[17] Ballard O, Morrow AL (2013) Human milk composition: nutrients and bioactive factors. Pediatr Clin North Am 60: 49-74
[18] Itoh Y, Kawamata Y, Harada M, et al. (2003) Free fatty acids regulate insulin secretion from pancreatic beta cells through GPR40. Nature 422: 173-176
[19] Briscoe CP, Tadayyon M, Andrews JL, et al. (2003) The orphan G protein-coupled receptor GPR40 is activated by medium and long chain fatty acids. J Biol Chem 278: 11303-11311
[20] Nauck M (2016) Incretin therapies: highlighting common features and differences in the modes of action of glucagon-like peptide-1 receptor agonists and dipeptidyl peptidase-4 inhibitors. Diabetes, obesity & metabolism 18: 203-216
[21] Ghislain J, Poitout V (2017) The Role and Future of FFA1 as a Therapeutic Target. Handb Exp Pharmacol 236: 159-180
[22] Hauge M, Vestmar MA, Husted AS, et al. (2015) GPR40 (FFAR1) - Combined Gs and Gq signaling in vitro is associated with robust incretin secretagogue action ex vivo and in vivo. Mol Metab 4: 3-14

[23] Rives ML, Rady B, Swanson N, et al. (2018) GPR40-Mediated Gα12 Activation by Allosteric Full Agonists Highly Efficacious at Potentiating Glucose-Stimulated Insulin Secretion in Human Islets. Mol Pharmacol 93: 581-591
[24] Oduori OS, Murao N, Shimomura K, et al. (2020) Gs/Gq signaling switch in β cells defines incretin effectiveness in diabetes. J Clin Invest 130: 6639-6655
[25] Wagner R, Kaiser G, Gerst F, et al. (2013) Reevaluation of fatty acid receptor 1 as a drug target for the stimulation of insulin secretion in humans. Diabetes 62: 2106-2111
[26] Buteau J (2008) GLP-1 receptor signaling: effects on pancreatic beta-cell proliferation and survival. Diabetes Metab 34 Suppl 2: S73-77
[27] Berger M, Scheel DW, Macias H, et al. (2015) Gαi/o-coupled receptor signaling restricts pancreatic β-cell expansion. Proceedings of the National Academy of Sciences of the United States of America 112: 2888-2893
[28] Brelje TC, Bhagroo NV, Stout LE, Sorenson RL (2008) Beneficial effects of lipids and prolactin on insulin secretion and beta-cell proliferation: a role for lipids in the adaptation of islets to pregnancy. J Endocrinol 197: 265-276
[29] Muzumdar MD, Tasic B, Miyamichi K, Li L, Luo L (2007) A global double-fluorescent Cre reporter mouse. Genesis 45: 593-605
[30] Gerst F, Kemter E, Lorza-Gil E, et al. (2021) The hepatokine fetuin-A disrupts functional maturation of pancreatic beta cells. Diabetologia 64: 1358-1374
[31] Steneberg P, Rubins N, Bartoov-Shifman R, Walker MD, Edlund H (2005) The FFA receptor GPR40 links hyperinsulinemia, hepatic steatosis, and impaired glucose homeostasis in mouse. Cell Metab 1: 245-258
[32] Fujiwara K, Maekawa F, Yada T (2005) Oleic acid interacts with GPR40 to induce Ca2+ signaling in rat islet beta-cells: mediation by PLC and L-type Ca2+ channel and link to insulin release. Am J Physiol Endocrinol Metab 289: E670-E677
[33] Schrage R, Schmitz AL, Gaffal E, et al. (2015) The experimental power of FR900359 to study Gq-regulated biological processes. Nat Commun 6: 10156
[34] Peterhoff M, Sieg A, Brede M, Chao CM, Hein L, Ullrich S (2003) Inhibition of insulin secretion via distinct signaling pathways in alpha2-adrenoceptor knockout mice. Eur J Endocrinol 149: 343-350
[35] Hammar E, Tomas A, Bosco D, Halban PA (2009) Role of the Rho-ROCK (Rho-associated kinase) signaling pathway in the regulation of pancreatic beta-cell function. Endocrinology 150: 2072-2079
[36] Ahrén B (2009) Islet G protein-coupled receptors as potential targets for treatment of type 2 diabetes. Nat Rev Drug Discov 8: 369-385
[37] Sassmann A, Gier B, Gröne HJ, Drews G, Offermanns S, Wettschureck N (2010) The Gq/G11-mediated signaling pathway is critical for autocrine potentiation of insulin secretion in mice. J Clin Invest 120: 2184-2193
[38] Pfeil EM, Brands J, Merten N, et al. (2020) Heterotrimeric G Protein Subunit Gαq Is a Master Switch for Gβγ-Mediated Calcium Mobilization by Gi-Coupled GPCRs. Mol Cell 80: 940-954.e946
[39] Bauer CS, Woolley RJ, Teschemacher AG, Seward EP (2007) Potentiation of exocytosis by phospholipase C-coupled G-protein-coupled receptors requires the priming protein Munc13-1. J Neurosci 27: 212-219
[40] Liu L, Dattaroy D, Simpson KF, et al. (2021) Gq signaling in α cells is critical for maintaining euglycemia. JCI Insight 6
[41] Svendsen B, Larsen O, Gabe MBN, et al. (2018) Insulin Secretion Depends on Intra-islet Glucagon Signaling. Cell reports 25: 1127-1134.e1122
[42] Peterhoff M, Sieg A, Brede M, Chao CM, Hein L, Ullrich S (2003) Inhibition of insulin secretion via distinct signaling pathways in alpha2-adrenoceptor knockout mice. European journal of endocrinology 149: 343-350
[43] Hauge-Evans AC, King AJ, Carmignac D, et al. (2009) Somatostatin secreted by islet delta-cells fulfills multiple roles as a paracrine regulator of islet function. Diabetes 58: 403-411

[44] Lorza-Gil E, Kaiser G, Rexen Ulven E, et al. (2020) FFA2-, but not FFA3-agonists inhibit GSIS of human pseudoislets: a comparative study with mouse islets and rat INS-1E cells. Sci Rep 10: 16497
[45] Vettor R, Granzotto M, De Stefani D, et al. (2008) Loss-of-function mutation of the GPR40 gene associates with abnormal stimulated insulin secretion by acting on intracellular calcium mobilization. The Journal of clinical endocrinology and metabolism 93: 3541-3550
[46] Diedisheim M, Oshima M, Albagli O, et al. (2018) Modeling human pancreatic beta cell dedifferentiation. Molecular metabolism 10: 74-86
[47] Puri S, Roy N, Russ HA, et al. (2018) Replication confers beta cell immaturity. Nature communications 9: 485
[48] Itoh Y, Kawamata Y, Harada M, et al. (2003) Free fatty acids regulate insulin secretion from pancreatic beta cells through GPR40. Nature 422: 173-176
[49] Hauke S, Keutler K, Phapale P, Yushchenko DA, Schultz C (2018) Endogenous Fatty Acids Are Essential Signaling Factors of Pancreatic beta-Cells and Insulin Secretion. Diabetes 67: 1986-1998
[50] Serra-Navarro B, Fernandez-Ruiz R, García-Alamán A, et al. (2021) Gsα-dependent signaling is required for postnatal establishment of a functional β-cell mass. Molecular metabolism 53: 101264

Figure Legend

Fig. 1 Effects of FFA1 deletion and parental HFD feeding blood parameters and insulin secretion in P6 and P11 offspring. (**a**) Experimental design. (**b**,**c**) Concentrations of blood glucose in (**b**) P6- and (**c**) P11-offspring. Results are expressed as mean ± SEM for n = 9-21 animals. (**d-g**) Insulin secretion from islets of (**d**,**f**) P6- and (**e**,**g**) P11-offspring isolated and incubated with test substances as described under Methods. Insulin secretion is expressed as mean ± SEM for the indicated number of replicates from n = 3 independent experiments. Black lines and dots represent data from WT, red lines and dots from FFA1 KO mice; white and grey bars represent parental CD and HFD, respectively. Significance between groups are as indicated. (**d**,**e**) *denotes significance to secretion at respective 2.8 mM glucose.

Fig. 2 FFA1 deletion and parental HFD increased expression of proliferation markers in P6-islets. (**a**) Heat map showing differentialy expressed genes in CD FFA1 KO P6-islets (DEG; $Log_2FC>1$ over WT; *p adj* <0.05). (**b**-**d**) Semiquantitative analysis of cellular mRNA levels of P6/P7- and adult offspring islets of WT (black line and dots) and FFA1 KO (red line and dots) progenitors fed CD (white columns) and HFD (grey columns). Results are given as mean ± SEM for n = 3-4 independent islet preparations. Significances between groups are as indicated. (**e**) Percentage of proliferative, Ki67-positive beta cells (GFP+) and (**f**) total beta cell mass (mg) assessed as described under Methods. Pancreatic sections (n = 4-8 for each animal) of n = 3-5 animals/group were examined. (**g**) Total pancreatic insulin content (µg/pancreas) during postnatal development of WT (black line and dots) and FFA1 KO (red line and dots) offspring animals from CD (white columns) and HFD (grey columns) fed progenitors. Results are expressed as mean ± SEM for n = 3-7 pancreata for each group. *, ** denotes significance vs respective P1; #, ## vs respective P11

Fig. 3 Effects of Gq inhibitors and of Gi/o inactivationon GSIS in P6-islets. (**a**-**c**,**e**) WT and (**d**,**f**) FFA1 KO P6-islets were isolated and incubated as described under Methods. Insulin secretion is expressed as mean ± SEM for the given number of replicates from n = 3-4 independent experiments. Significances are as indicated; FR900359, FR900; pertussis toxin, PTX; YM254890, YM; exendin-4, Ex-4

Fig. 4 Effects of RhoA and ROCK inhibition on GSIS in WT and KO P6-islets. (**a**,**c**) FFA1 KO and (**b**,**d**) WT P6-islets were isolated and incubated as described under Methods. Test substances were added at the indicated concentrations. Results are expressed as mean ± SEM for the given number of observations from n = 3-7 independent experiments. Significances are as indicated. **(e)** WT P6-islet cells were isolated and cultured as described under Methods. H1152 (1µM) was added for 1h in cell culture. The cells were stained for actin (phalloidin, red) and insulin (anti-insulin Ab, magenta)

Fig. 5 GSIS of INS-1E cells depends on Gq. (**a**-**d**) INS-1E cells were cultured at 11 mM glucose, incubated, transfected and cellular proteins extracted as described under Methods. (**a**) Relative mRNA levels of *Gnaq* (ΔCt against *Rps13*) assessed by RT-PCR and (**b**,**c**) protein level of Gq upon treatment wit non-targering and anti-Gnaq siRNA. Results are expressed as mean ± SEM of n = 3 independent experiments. (**d**,**e**) Insulin secretion of (**d**) INS1-E cells upon treatment wit non-targering and Gnaq siRNA and (**e**) INS-1E cells treated with the Gq inhibitor FR900359 as described under methods. Results are expressed as mean±SEM of n = 3-6 independent experiments and significances are as indicated. (**f**) Representative confocal images of INS-1E cells immunostained for Gq (green) and treated as described under Methods. Nuclei were stained with DAPI (blue).

Fig. 6 Effects of Gq inhibitor FR900359 on GSIS and cytosolic $[Ca^{2+}]_i$ in adult islets. (**a,b**) Adult WT islets were isolated and incubated as described under Methods. Insulin secretion is expressed as mean ± SEM for the given number of replicates from n = 3 independent experiments. (**c**-**f)** Cytosolic Ca^{2+} was assessed with FURA-2 in mouse islets. (**c**,**e**) Traces of cytosolic $[Ca^{2+}]_i$ oscillations in isolated islets of adult (12 weeks old) mice cultured and treated as described under Methods. The islets were (**c**,**d**) preincubated for 1 h with FR900359 before the recording was started or (**e**,**f**) acutely treated with FR900350 during FURA2 recording (**d**,**f**) Area under the curve (AUC) of cytosolic $[Ca^{2+}]_i$ expressed as mean ± SEM for the given number of observations from n = 4 independent experiments.

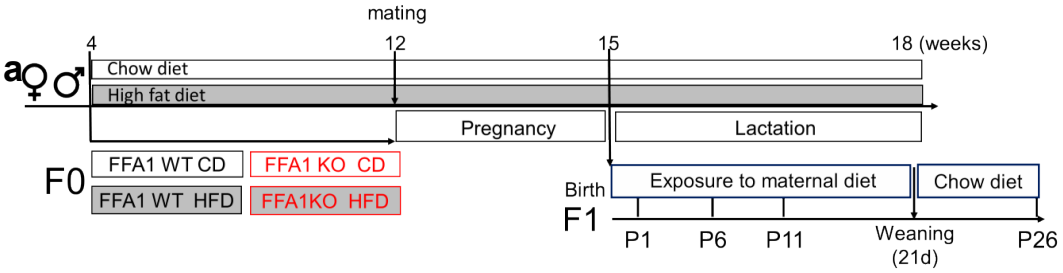
mating
4
12
15
18 (weeks)
a♀♂
Chow diet
High fat diet
Pregnancy
Lactation
F0
FFA1 WT CD
FFA1 KO CD
FFA1 WT HFD
FFA1KO HFD
Birth
F1
Exposure to maternal diet
Chow diet
P1
P6
P11
Weaning
(21d)
P26

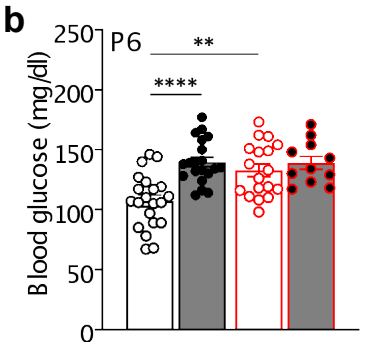
b
P6
Blood glucose (mg/dl)
250
200
150
100
50
0
**
****

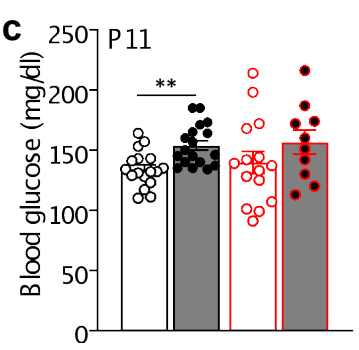
c
P11
Blood glucose (mg/dl)
250
200
150
100
50
0
**

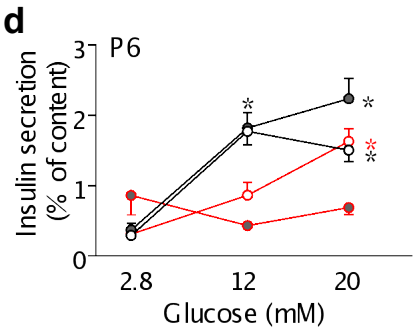
d
P6
Insulin secretion
(% of content)
3
2
1
0
2.8
12
20
Glucose (mM)

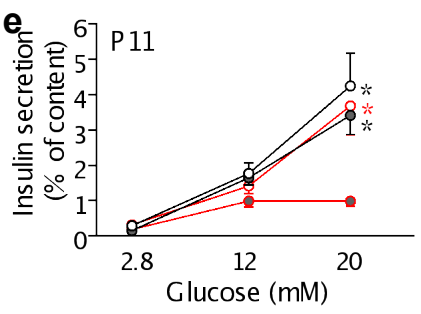
e
P11
Insulin secretion
(% of content)
6
5
4
3
2
1
0
2.8
12
20
Glucose (mM)

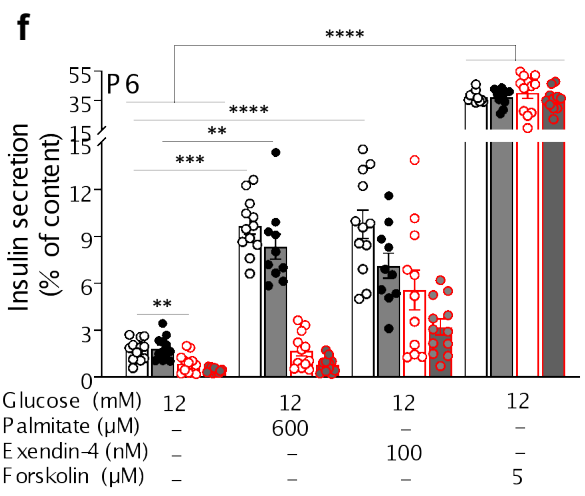
f
P6
Insulin secretion
(% of content)
55
35
15
12
9
6
3
0
****
****
**
***
**
Glucose (mM) 12 12 12 12
Palmitate (μM) – 600 – –
Exendin-4 (nM) – – 100 –
Forskolin (μM) – – – 5

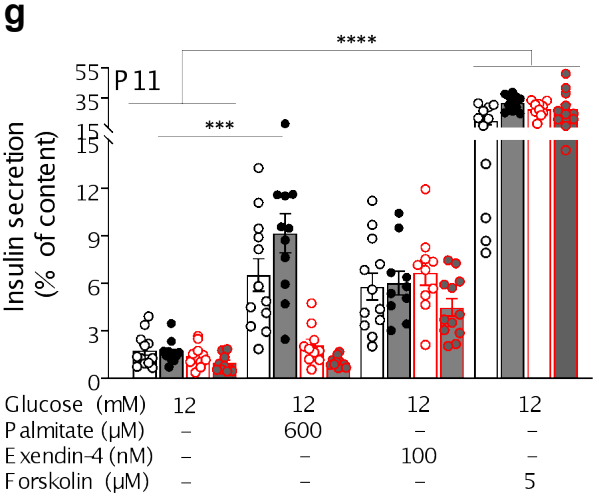
g
P11
Insulin secretion
(% of content)
55
35
15
12
9
6
3
0
****
***
Glucose (mM) 12 12 12 12
Palmitate (μM) – 600 – –
Exendin-4 (nM) – – 100 –
Forskolin (μM) – – – 5

Fig. 1

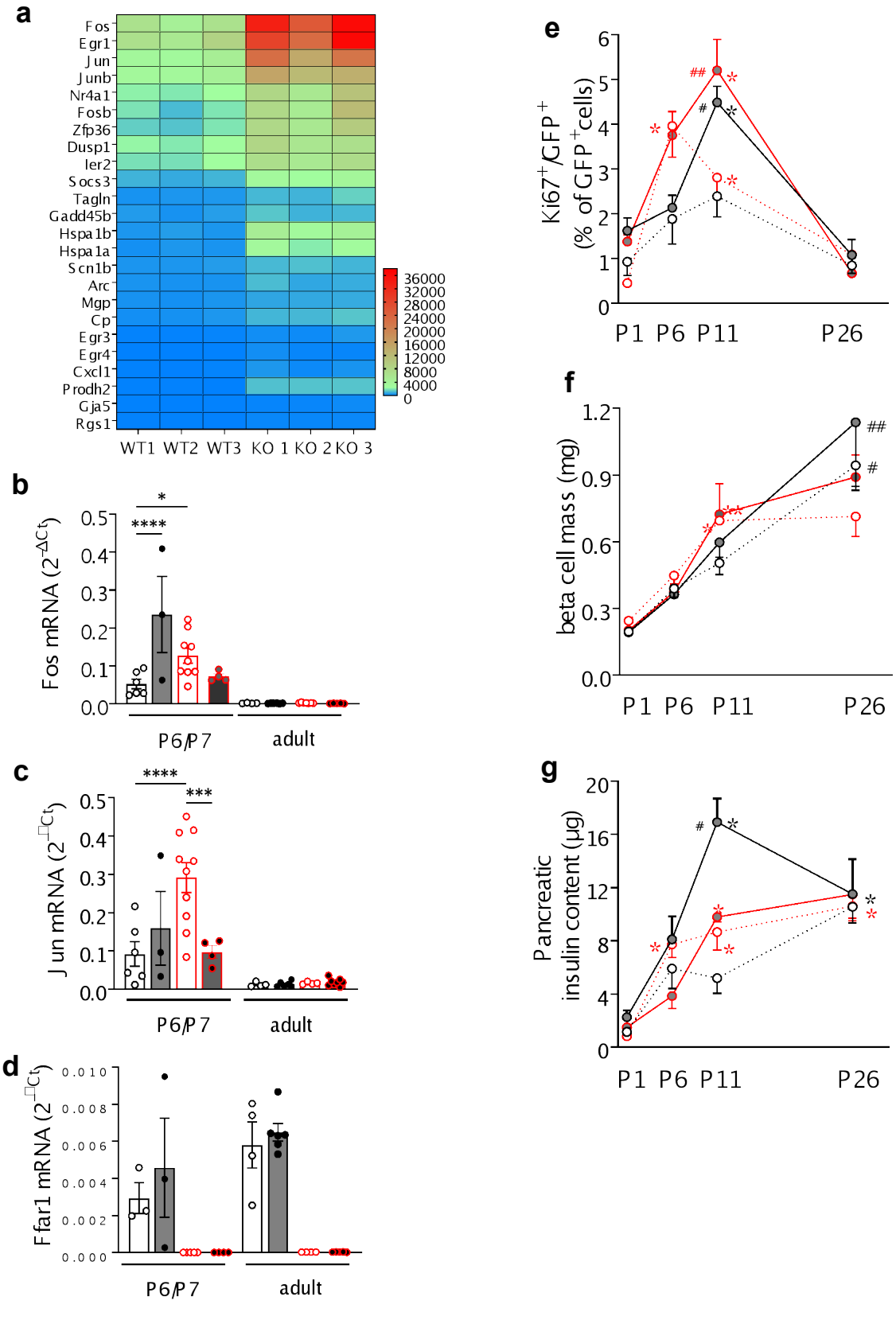
a
Fos
Egr1
Jun
Junb
Nr4a1
Fosb
Zfp36
Dusp1
Ier2
Socs3
Tagln
Gadd45b
Hspa1b
Hspa1a
Scn1b
Arc
Mgp
Cp
Egr3
Egr4
Cxcl1
Prodh2
Gja5
Rgs1
WT1 WT2 WT3 KO 1 KO 2 KO 3
36000
32000
28000
24000
20000
16000
12000
8000
4000
0
b
Fos mRNA (2^-ΔCt)
P6/P7
adult
c
Jun mRNA (2^-□Ct)
P6/P7
adult
d
Ffar1 mRNA (2^-□Ct)
P6/P7
adult
e
Ki67+/GFP+ (% of GFP+cells)
P1 P6 P11 P26
f
beta cell mass (mg)
P1 P6 P11 P26
g
Pancreatic insulin content (µg)
P1 P6 P11 P26

Fig. 2

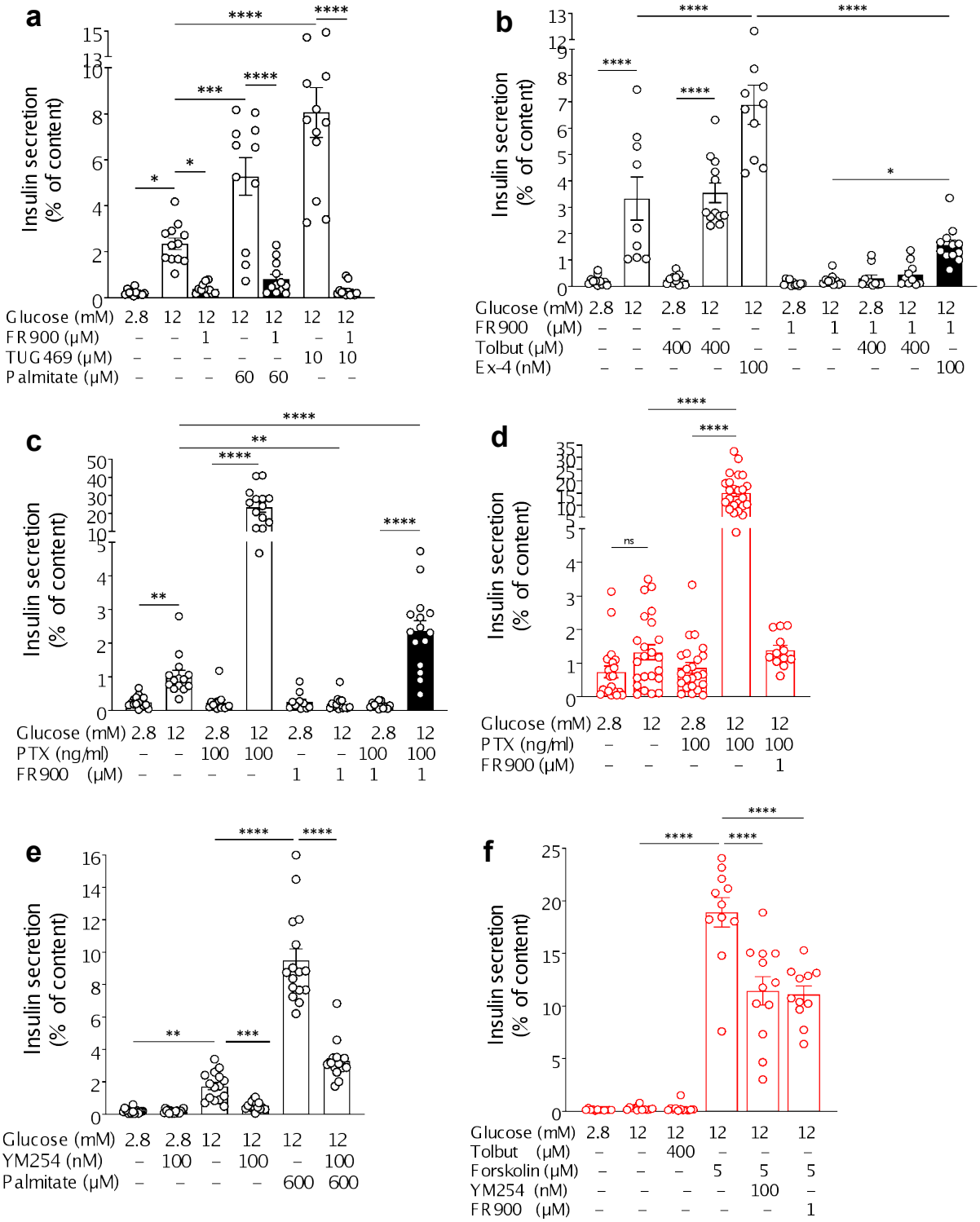
a
Insulin secretion (% of content)
Glucose (mM) 2.8 12 12 12 12 12 12
FR900 (μM) – – 1 – 1 – 1
TUG469 (μM) – – – – – 10 10
Palmitate (μM) – – – 60 60 – –
b
Insulin secretion (% of content)
Glucose (mM) 2.8 12 2.8 12 12 2.8 12 2.8 12 12
FR900 (μM) – – – – – 1 1 1 1 1
Tolbut (μM) – – 400 400 – – – 400 400 –
Ex-4 (nM) – – – – 100 – – – – 100
c
Insulin secretion (% of content)
Glucose (mM) 2.8 12 2.8 12 2.8 12 2.8 12
PTX (ng/ml) – – 100 100 – – 100 100
FR900 (μM) – – – – 1 1 1 1
d
Insulin secretion (% of content)
ns
Glucose (mM) 2.8 12 2.8 12 12
PTX (ng/ml) – – 100 100 100
FR900 (μM) – – – – 1
e
Insulin secretion (% of content)
Glucose (mM) 2.8 2.8 12 12 12 12
YM254 (nM) – 100 – 100 – 100
Palmitate (μM) – – – – 600 600
f
Insulin secretion (% of content)
Glucose (mM) 2.8 12 12 12 12 12
Tolbut (μM) – – 400 – – –
Forskolin (μM) – – – 5 5 5
YM254 (nM) – – – – 100 –
FR900 (μM) – – – – – 1

Fig. 3

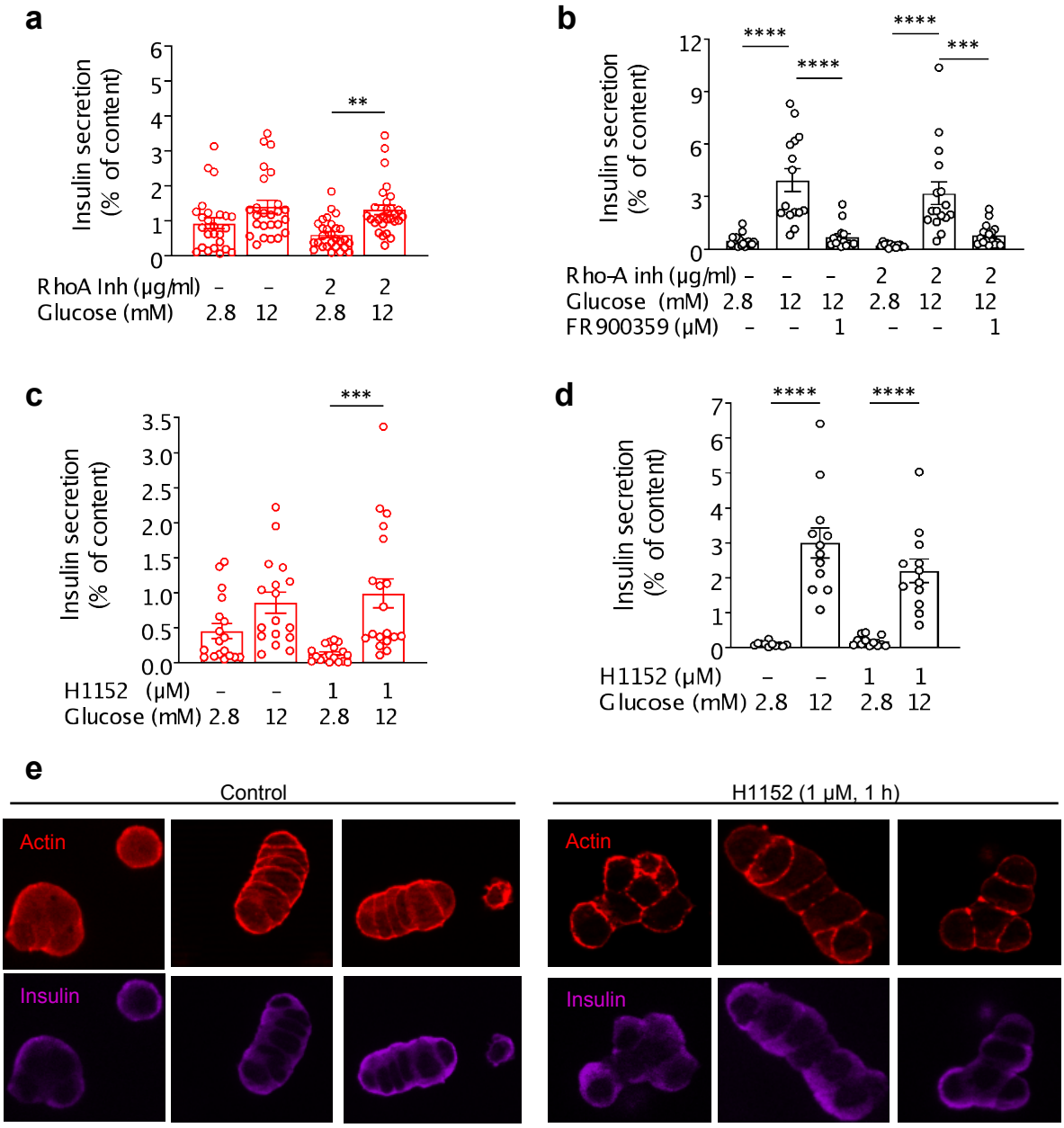
a
Insulin secretion (% of content)
RhoA Inh (µg/ml) – – 2 2
Glucose (mM) 2.8 12 2.8 12
b
Insulin secretion (% of content)
Rho-A inh (µg/ml) – – – 2 2 2
Glucose (mM) 2.8 12 12 2.8 12 12
FR900359 (µM) – – 1 – – 1
c
Insulin secretion (% of content)
H1152 (µM) – – 1 1
Glucose (mM) 2.8 12 2.8 12
d
Insulin secretion (% of content)
H1152 (µM) – – 1 1
Glucose (mM) 2.8 12 2.8 12
e
Control
H1152 (1 µM, 1 h)
Actin
Insulin

Figure 4

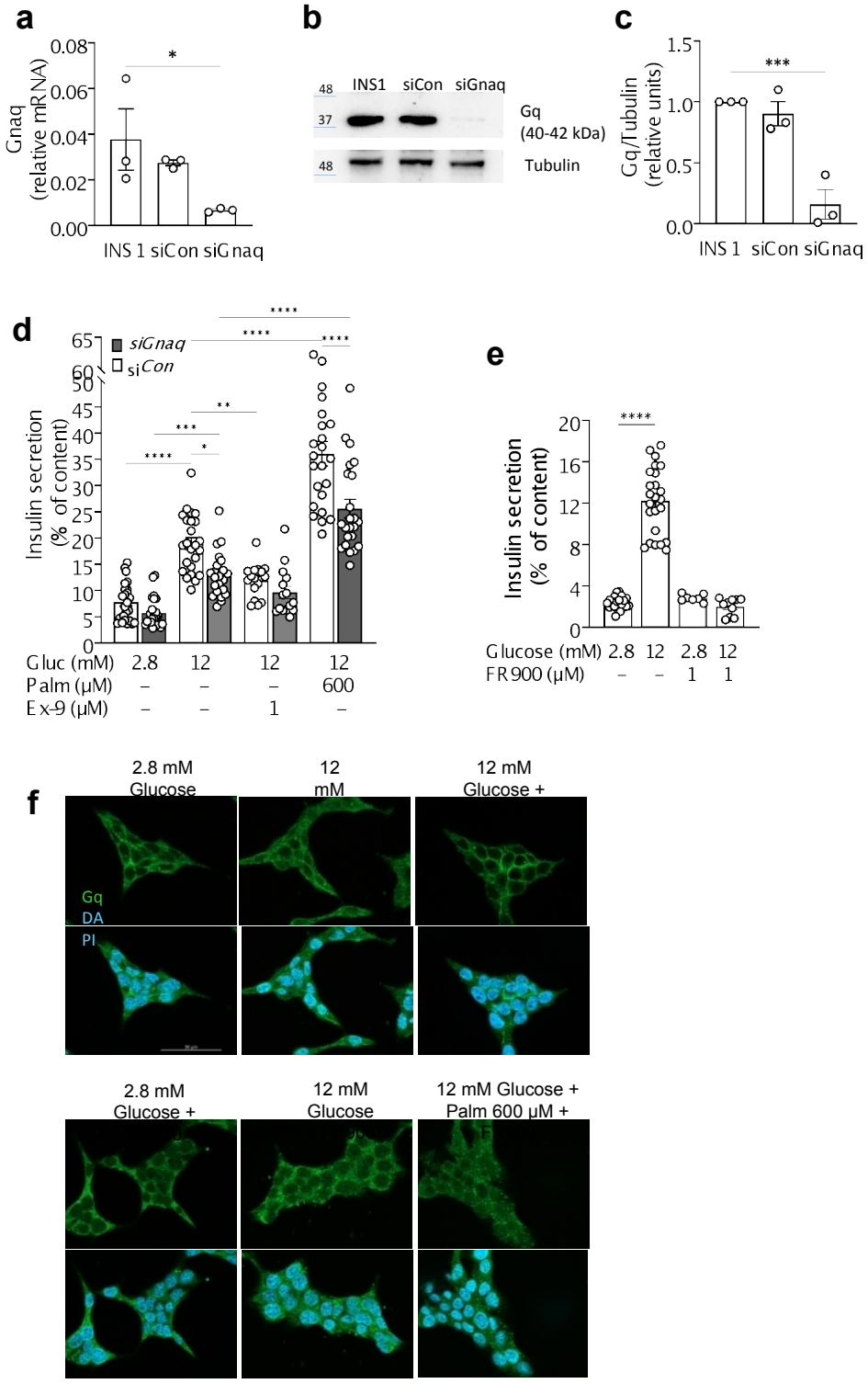
a
Gnaq (relative mRNA)
0.08
0.06
0.04
0.02
0.00
*
INS 1 siCon siGnaq
b
48
37
48
INS1 siCon siGnaq
Gq (40-42 kDa)
Tubulin
c
Gq/Tubulin (relative units)
1.5
1.0
0.5
0.0
***
INS 1 siCon siGnaq
d
siGnaq
siCon
Insulin secretion (% of content)
65
60
50
45
40
35
30
25
20
15
10
5
0
****
****
****
**
***
*
****
Gluc (mM) 2.8 12 12 12
Palm (μM) – – – 600
Ex-9 (μM) – – 1 –
e
Insulin secretion (% of content)
20
16
12
8
4
0
****
Glucose (mM) 2.8 12 2.8 12
FR900 (μM) – – 1 1
f
2.8 mM Glucose
12 mM
12 mM Glucose +
Gq
DA
PI
2.8 mM Glucose +
12 mM Glucose
12 mM Glucose + Palm 600 μM +

Fig. 5

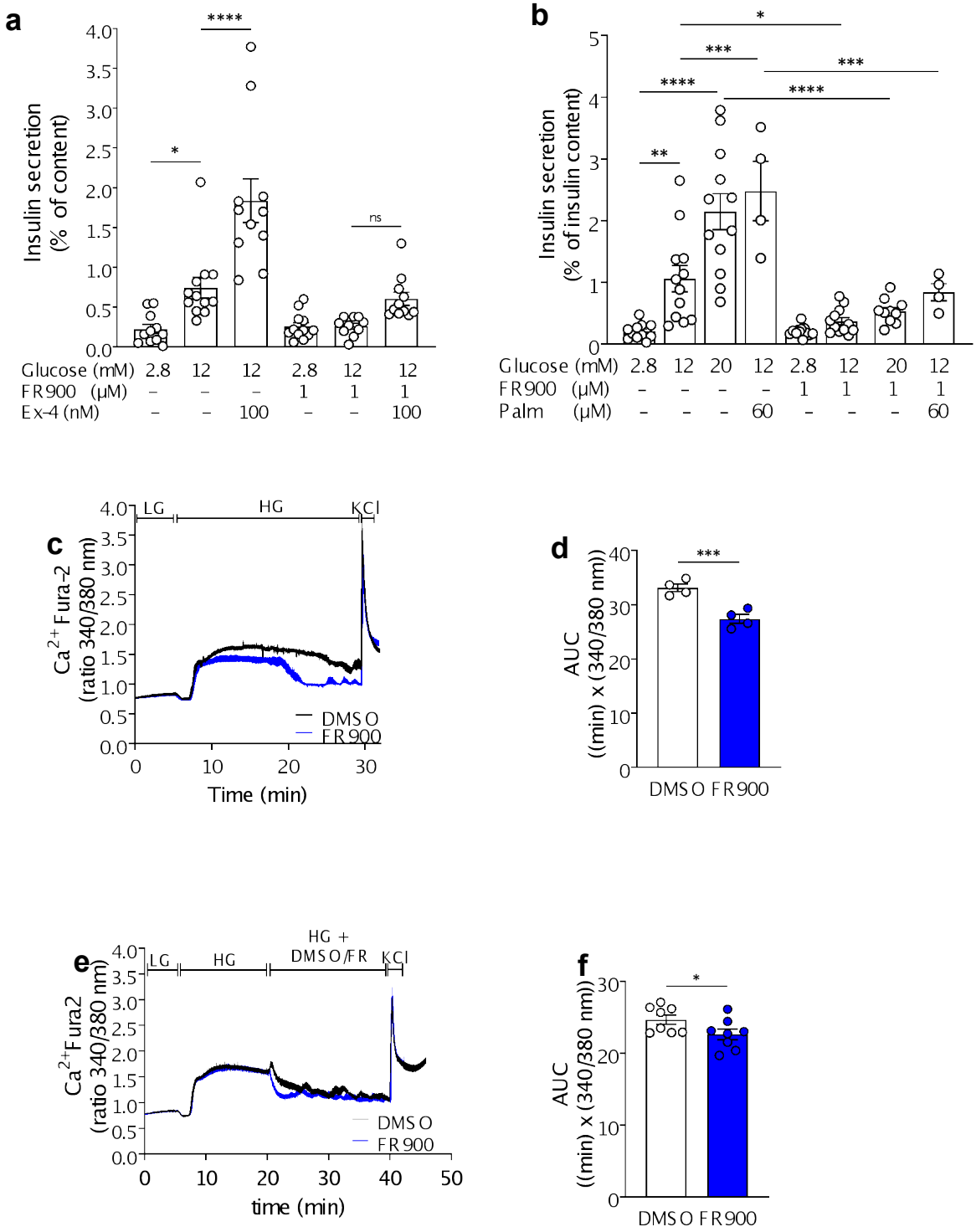
a
Insulin secretion (% of content)
Glucose (mM) 2.8 12 12 2.8 12 12
FR900 (μM) – – – 1 1 1
Ex-4 (nM) – – 100 – – 100
b
Insulin secretion (% of insulin content)
Glucose (mM) 2.8 12 20 12 2.8 12 20 12
FR900 (μM) – – – – 1 1 1 1
Palm (μM) – – – 60 – – – 60
c
LG
HG
KCl
Ca2+ Fura-2 (ratio 340/380 nm)
DMSO
FR900
Time (min)
d
AUC ((min) x (340/380 nm))
DMSO FR900
e
LG
HG
HG + DMSO/FR
KCl
Ca2+Fura2 (ratio 340/380 nm)
DMSO
FR900
time (min)
f
AUC ((min) x (340/380 nm))
DMSO FR900

Figure 6

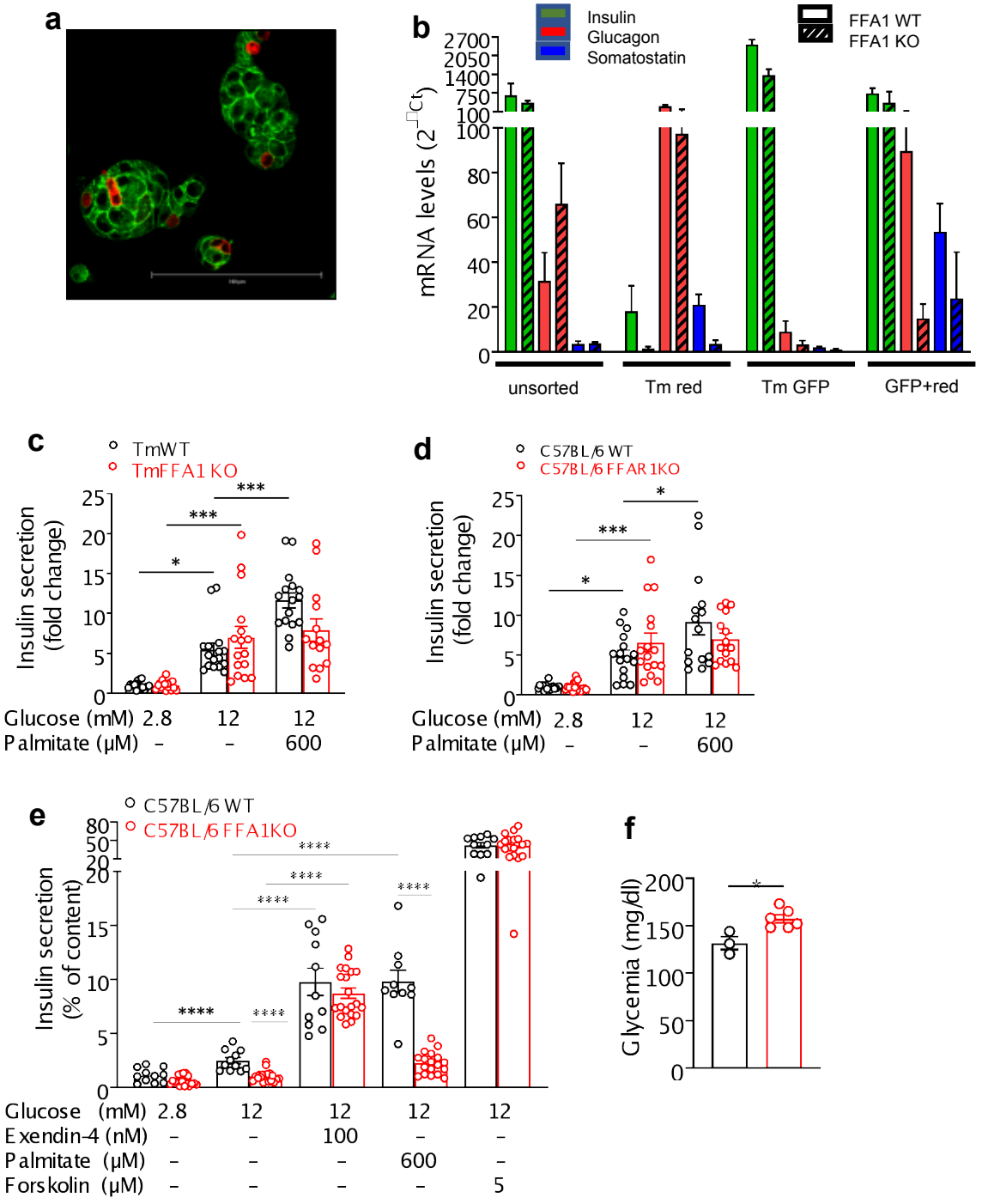

ESM Fig. 1 The transgenic RIP-Cre ROSA mTmG mouse islets display similar regulation of insulin secretion as C57BL/6 mouse islets.

(**a**) Isolated islet cell clusters of ROSA mTmG mice displaying green and red fluorescent cells. (**b**) Relative mRNA levels in un-/sorted green and red fluorescent islet cells of ROSA mTmG mice. (**c-e**) Insulin secretion in isolated islets from (**c**) adult mT/mG FFA1 WT (black) and FFA1 KO (red) (**d**) adult C57BL/6 FFA1 WT (black) and FFA1 KO (red) and (**e**) 6 d old C57BL/6 WT and FFA1 KO littermates. (**f**) Fed plasma glucose of 6 d old C57BL/6 WT and FFA1 KO littermates. Results are expressed as mean ± SEM for the given number of observation of n=3-6 independent experiments. Significant effects between groups as indicated

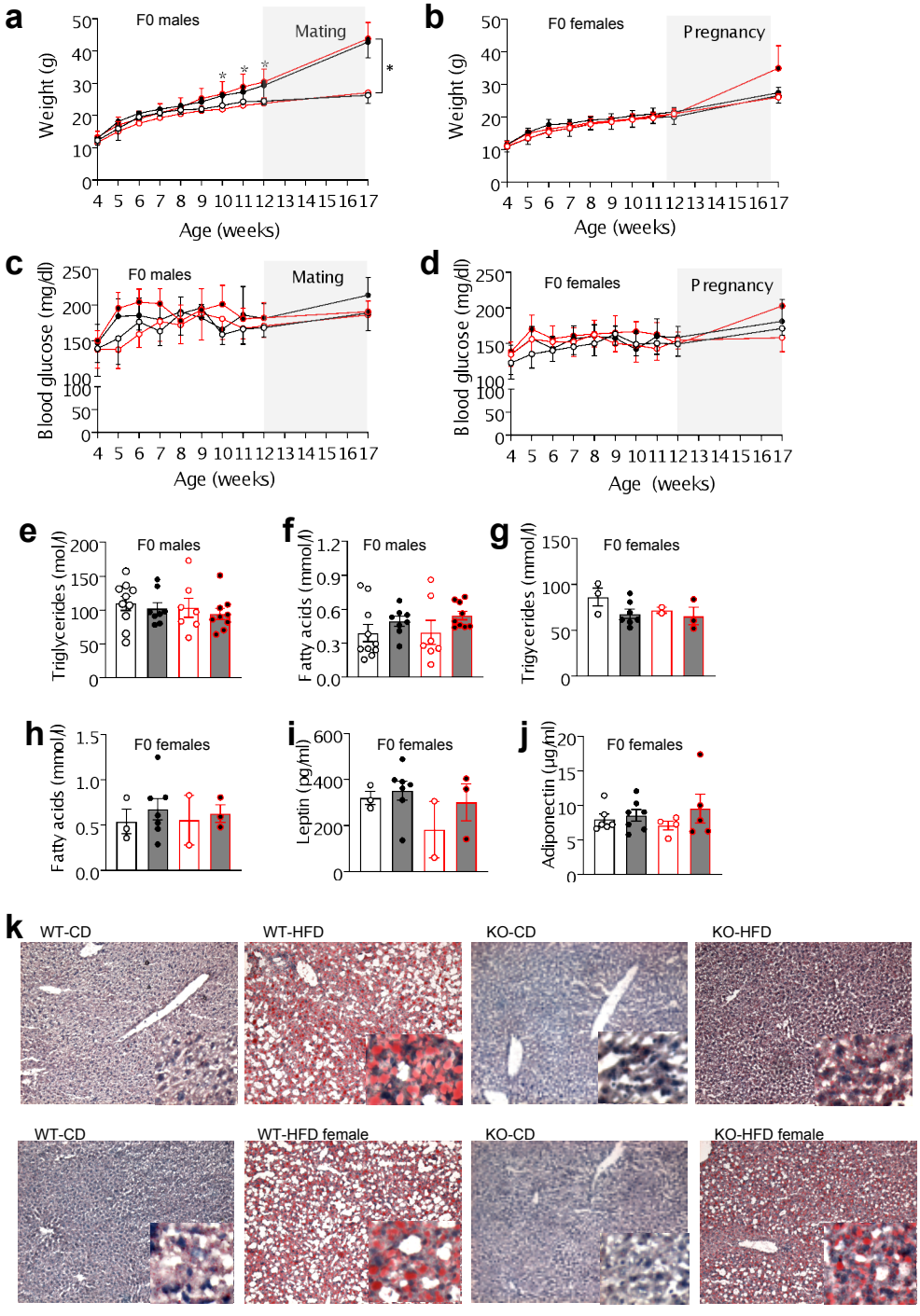

ESM Fig. 2 Effect of HFD on metabolic parameters in F0 (parental) generation.
Weight gain and blood glucose concentrations of WT (black lines) and FFA1 KO (red lines) (**a**,**c**) male and (**b**,**d**) female mice fed chow (white dots) or high fat (black dots) diet. Serum triglycerides and NEFAs in (**e**,**f**) male and (**g**,**h**) female mice and (**i**,**j**) leptin and adiponectin levels in female mice of F0 generation. (**k**) Liver steatosis detected with oil red staining in 10 µm thick cryosections of mouse livers collected at the end of the feeding period. Results are expressed as mean ± SEM for n=8-15 mice/group; Note that FFA1 KO mice fed HFD display less liver fat droplets than WT mice as previously described (ref 31).

n=8-15
ANOVA one-way Tukey's
*p<0.05

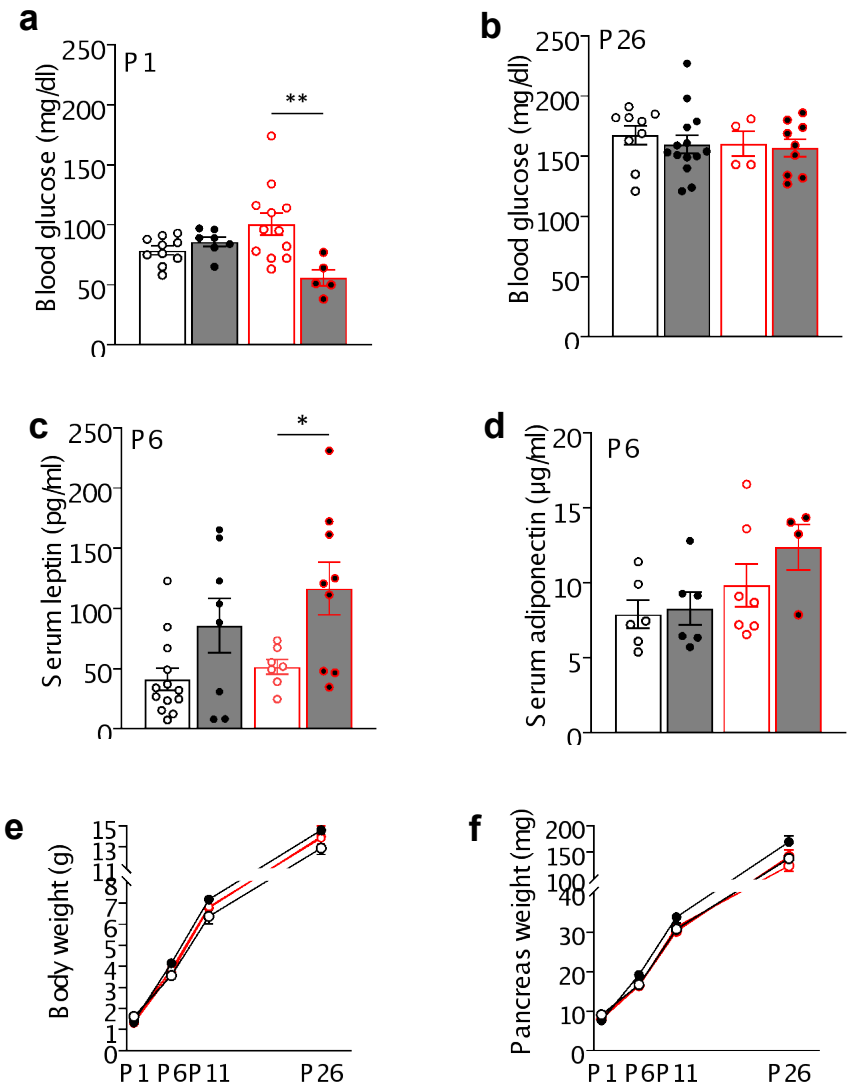

ESM Fig. 3 Effects of *Ffar1* deletion and parental HFD feeding on offspring blood parameters, body weight and pancreatic weight. Concentrations of (**a**,**b**) blood glucose, serum (**c**) leptin and (**d**) adiponectin in (**a**) P1-, (**b**) P26- and (**c**,**d**) P6-offspring. (**e**) Body weight and (**f**) pancreas weight of P1-P26 offspring. Results are expressed as mean ± SEM for n = 4-22 offspring animals. Black lines and dots represent data from WT, red lines and dots from FFA1 KO mice, white and grey bars from CD and HFD offspring, respectively.

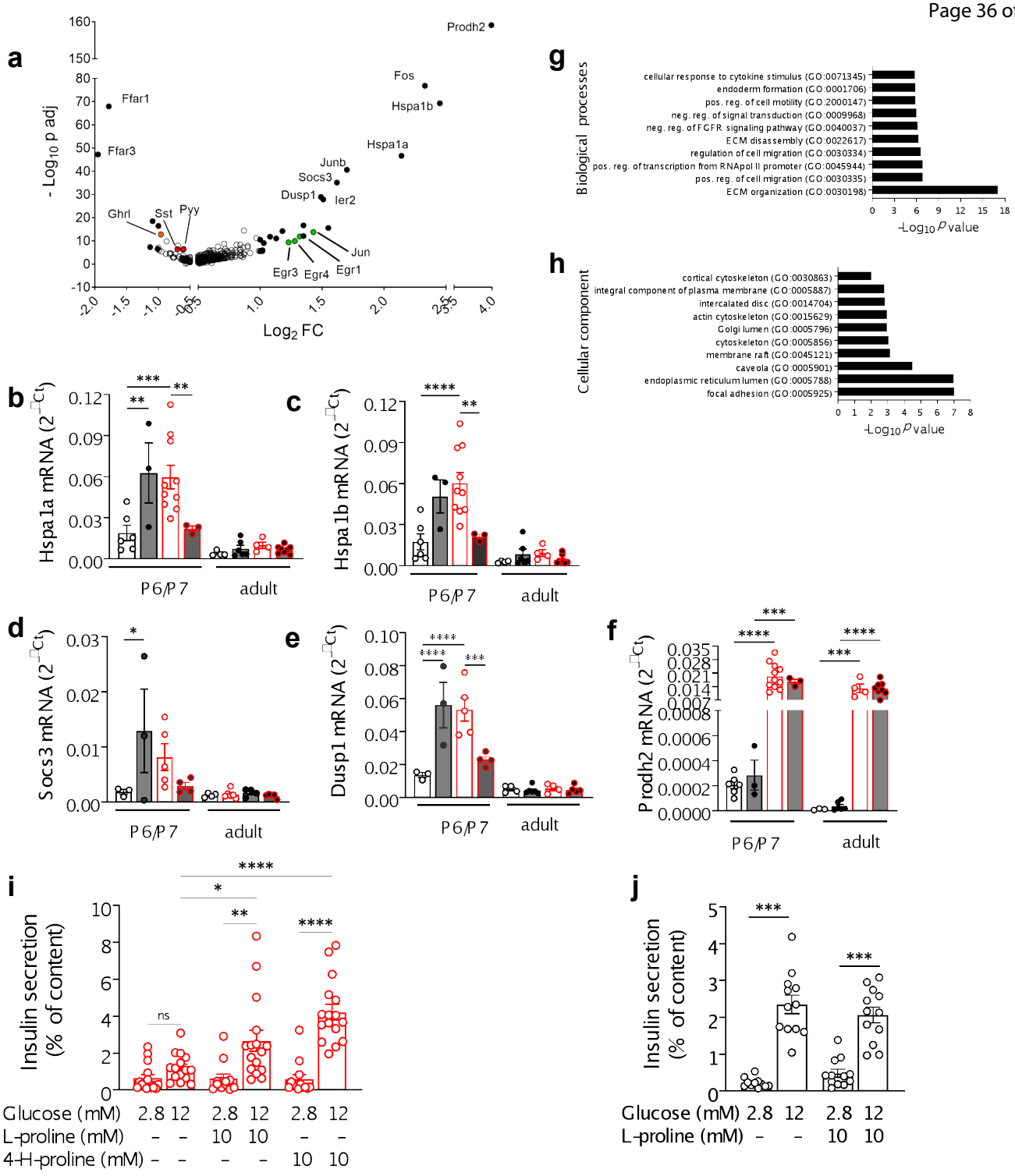

ESM Fig. 4 Transcriptome analysis and GSIS of WT and FFA1 KO P6-islets.
(**a**) Volcano plot showing differentially expressed genes (DEG; -0.5>Log_2FC>+0.5; p adj <0.05) in FFA1 KO vs WT P6-islets. Black dots are up- and downregulated (-1>Log_2FC>+1) genes in KO P6-islets. (**b**-**f**) Semiquantitative analysis of cellular mRNA levels of P6/P7- and adult islets from WT (black line and dots) and FFA1 KO (red line and dots) offspring from CD (white columns) and HFD fed (grey columns) progenitors. Results are given as mean±SEM for n=3-4 independent islet preparations. (**g**,**h**) Gene ontology (GO) enrichment analysis of DEGs (-0.5>Log2FC>+0.5; p adj <0.05) from FFA1 KO P6-islets (**i**,**j**) GSIS of (**i**) FFA1 KO and (**j**) WT P6-islets. Results are experssed as mean ± SEM for the given number of observation from n = 3-5 independent experiments. Significances are as indicated

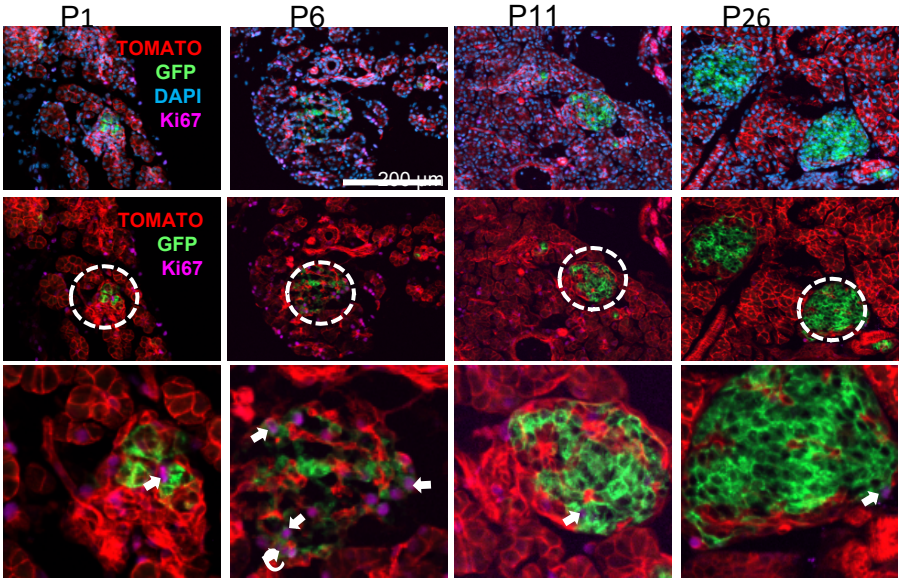

ESM Fig. 5 Proliferative beta cells detected by Ki67 immunostaining (magenta) in pancreatic sections of P1-P26 offspring. The insulin producing cells express GFP (green fluorescence; see ESM Fig. 1b). Note the high number of proliferating cells in the exocrine ares (Tomato, red fluorescence) of the pancreatic sections. White arrowheads indicate proliferative beta cells.

ESM Methods

Mouse model and diet feeding

C57BL/6 (Gt(ROSA)26Sor$^{tm4\ (ACTB\text{-}tdTomato,\text{-}EGFP)Luo}$) were bred with RIP-cre mice (Tg(Ins2-cre)23Herr) on a C57BL/6 background to generate C57BL/6-RIP-Cre Tomato mice. The ROSA mTmG mice possess loxP sites on each side of a membrane-targeted tdTomato (mT) cassette and have red fluorescent tissues [29]. In the RIP-Cre Tomato mice, the cells expressing Cre recombinase, i.e. insulin producing cells have plasma membrane-localized EGFP (mG) which replaces the red fluorescent mT (ESM Fig. 1a-b). RIP-CreTomato mice were bred with Ffar1^{tm1Heed} mice to create C57BL/6-RipCre-ROSA$^{mT/mG}$ WT and FFA1 KO animals. Mice were kept on a 12 h day-night cycle with free access to water and regular chow diet. The chow diet (CD, # D12450B) contained 10 kcal% fat, while high fat diet (HFD; #D12451, Research Diets Inc, USA) contained 45 kcal% fat.

Measurement of blood parameters

Blood glucose was measured using a glucose analyzer (Accu-Chek; Roche Diagnostics, Germany). Serum insulin, leptin and adiponectin were measured using ultrasensitive insulin (#10-1247-10; Mercodia, Sweden), leptin and adiponectin (#RAB0334 and #RAB1115; Millipore Saint Louis, USA) ELISA kits respectively. Serum NEFAs were determined using a free fatty acid quantification kit (MAK044, Sigma-Aldrich, Germany). Serum triglycerides were assessed using ADVIA® TRIG reagents (Siemens Healthcare Diagnostics Inc., Tarrytown NY, USA).

Mouse islet isolation and culture

Isolated islets were whashed in Hank's balanced salt solution containing (in mM): 137 NaCl, 5 KCl, 1.25 CaCl2, 0.81 MgSO4, 1.2 Na2HPO4, 0.44 KH2PO4, 4 NaHCO3, 10 Hepes pH 7.25 , 2.8 glucose and 2.25 mg/ml BSA (fraction V, #A3294; Sigma).

Isolated islets were cultured in RPMI1640 medium containing 5 mM glucose and supplemented with 10 % FCS, 10 mM HEPES, 2 mM L-glutamine, 1 mM Na-pyruvate.

INS-1E cell culture, siRNA treatment, RNA isolation and Western blotting

INS-1E cells were cultured in RPRMI1640 containing 11 mM glucose, 10 % FCS, 10 mM HEPES, 2 mM L-glutamine, 1 mM Na-pyruvate and 0.05 mM 2-mercaptoethanol.

The cells were transfected with 20 nM non-targeting siRNA (#D-001810-10) or Gnaq siRNA (L-092425; Dharmacon) using DharmaFect3 (#T-2003;Darmacon) and were kept 3 d in culture before further analysis.

For protein lysates, INS-1E cells were lysed in RIPA buffer containing (in mmol/l): 25 Tris/HCl (pH 7.5), 150 NaCl, 2 EDTA, 10 NaF, 1 Na3VO4, and 10 % glycerol, 1 % Nonidet-P40, 0.1 % SDS, 0.1 % C24H39NaO4 and protease inhibitors as described previously (30).

Insulin secretion

Krebs Ringer buffer (KRB) contains (in mM): 135 NaCl, 4.8 KCl, 1.2 Mg_2SO_4, 1.2 KH_2PO_4, 2.6 $CaCl_2$, 5 $NaHCO_3$, 10 HEPES (pH 7.4), 0.5 % BSA and 2.8 mM glucose. Insulin was measured with ELISA kit (#10-1247-01; Mercodia, Sweden).

Drugs were purchased as indicated: pertussis toxin (P7208; Merck); palmitic acid (#P0500; Sigma), TUG-469 (synthesized and provided by ERU and TU); exendin-4 (#E7144; Merck); forskolin (#F3917; Merck); FR900359 (Gq inhibitor, characterized and provided by EK); YM-254890 (Gq inhibitor, #10-1590; Focus Biomolecules), H1152 (#SYN1221; AdipoGen) CT3 toxin (#CT04; Cytoskeleton).

FACS sorting of GFP- and tdTomato-fluorescent cells

Isolated islets were digested with trypsin to single cell suspension. Fluorescent activated cell sorting (FACS) was performed with a BD FACS Aria cell sorter (BD Biosciences; Heidelberg) using BD Diva Software. Islet cells were separated intogreen (beta cells) and red (non-beta cells) fluorescent fractions. Successful separation of beta from non-beta cells was confirmed by the assessment of relative mRNA levels of insulin, glucagon and somatostatin using RT-PCR (ESM Fig. 1b).

Antibodies

The antibodies used are as following: anti-Ki67 antibody (#ab15580, abcam), nti-rabbit IgG crossed adsorbed secondary antibody Alexa-Fluor 633 (#A-21070; Invitrogen), anti-rabbit IgG cross-adsorbed secondary antibody Alexa Fluor 488 (#A-11008; Invitrogen); anti-Gq antibody (#ab210004, abcam); anti-rabbit IgG HRP coupled antibody (#31460; Invitrogen).

Cytosolic Ca^{2+} measurement

Isolated islets were whashed and incubated in KRB-Henseleit solution (KHB) containing (in mM): 120 NaCl, 4.8 KCl, 1.2 $MgCl_2$, 2.5 $CaCl_2$, 24 $NaHCO_3$, 5 HEPES (pH 7.4), 2.8 glucose and 0.1% BSA.

WB for Gq / Tubulin

INS-1E cells: untranfected and transfected with siCon/siGnaq